Supplementary Information for

Development of a Xanthene-Based NIR Fluorescent Probe for Accurate and Sensitive Detection of γ-Glutamyl Transpeptidase in Cancer Diagnosis and Treatment

Chia-Kai Lai [a], Kuppan Magesh [b], Sivan Velmathi[b] and Shu-Pao Wu[a,*]

[a] Department of Applied Chemistry, National Yang Ming Chiao Tung University, Hsinchu, ROC, Taiwan

[b] Department of Chemistry, National Institute of Technology, Tiruchirappalli, India

* Corresponding authors.

spwu@nycu.edu.tw (S. Wu)

Contents

13. **Figure S3** (a) The fluorescence intensity at 648 nm of fluorophore **XM-OH** (0 ~ 12 μM) in DMSO- H_2O (v/v = 4/6, 6 mM PBS, pH 7.4) solution. (b) Lineweaver-Burk plot of probe **XM-Glu** in response to GGT (100 mU/mL). λ_{ex}= 595 nm
14. **Figure S4** The fluorescence changes of **XM-Glu** (20 μM), and **XM-Glu** (20 μM) with GGT (100 mU/mL) in different pH value of DMSO-H_2O (v/v = 4/6, 6 mM PBS) solution for 4 h. λ_{ex} = 595 nm.
15. **Figure S5** HPLC chromatograms of fluorophore **XM-OH** (100 μM), probe **XM-Glu** (100 μM), and **XM-Glu** (100 μM) + GGT (400 mU/mL). The absorption peak was measured at 520 nm. (HPLC conditions: 0 min: 80% H_2O + 20% MeOH, 5 ~ 15 min: 4.5 % H_2O + 95.5% MeOH, 20 min: 100% MeOH)
16. **Figure S6** ESI-MS spectra of **XM-Glu** reacted with GGT.
17. **Figure S7** Cell viability of HepG2 and HEK293 cells treated with **XM-Glu** (0, 5, 10, 15, 20, 25 μM) at 37°C for 24 h. The results are the mean and standard deviation of three independent experiments.
18. **Figure S8** Fluorescence images of HeLa cells. (a ~ d) Control group. (e ~ h) HeLa cells were incubated with **XM-Glu** (10 μM) at 37°C for 2 h (Blue fluorescence: λ_{ex} = 405 nm. λ_{em} = 435 ~ 485 nm. Red fluorescence: λ_{ex} = 561 nm. λ_{em} = 600 ~ 700 nm.)
19. **Figure S9** Fluorescence images of HEK293 cells. Control group (a–d). Experimental group treated with **XM-Glu** (10 μM) at 37°C for 2 hours (e–h). DAPI fluorescence: Excitation wavelength = 405 nm, Emission wavelength = 435–485 nm. Red fluorescence: Excitation wavelength = 561 nm, Emission wavelength = 600–700 nm.
20. **Figure S10** Fluorescence intensity at tumor site pre-injection, 5 min after injection, 1 h after injection, and 2 h after injection.
21. **Figure S11** (a) Fluorescence imaging of tissue sections from tumors and organs of mouse incubated with **XM-Glu** (50 μM) for 2 h. Fluorescence: λ_{ex} = 545 nm. λ_{em} = 590 ~ 650 nm. (b) Relative intensity plots of the images.
22. **Figure S12** ^{1}H NMR (400 MHz) spectrum of Compound **1** in $CDCl_3$.
23. **Figure S13** ^{13}C NMR (100 MHz) spectrum of Compound **1** in $CDCl_3$
24. **Figure S14** ^{1}H NMR (400 MHz) spectrum of Compound **2** in $CDCl_3$.
25. **Figure S15** ^{13}C NMR (100 MHz) spectrum of Compound **2** in $CDCl_3$.
26. **Figure S16** FD mass spectrum of compound **2**.
27. **Figure S17** ^{1}H NMR (400 MHz) spectrum of Compound **3** in $CDCl_3$.
28. **Figure S18** ^{13}C NMR (100 MHz) spectrum of Compound **3** in $CDCl_3$.
29. **Figure S19** FD mass spectrum of compound **3**
30. **Figure S20** ^{1}H NMR (400 MHz) spectrum of **XM-OH** in DMSO-d_6.
31. **Figure S21** ^{13}C NMR (150 MHz) spectrum of **XM-OH** in DMSO-d_6.

Synthesis of probe XM-Glu

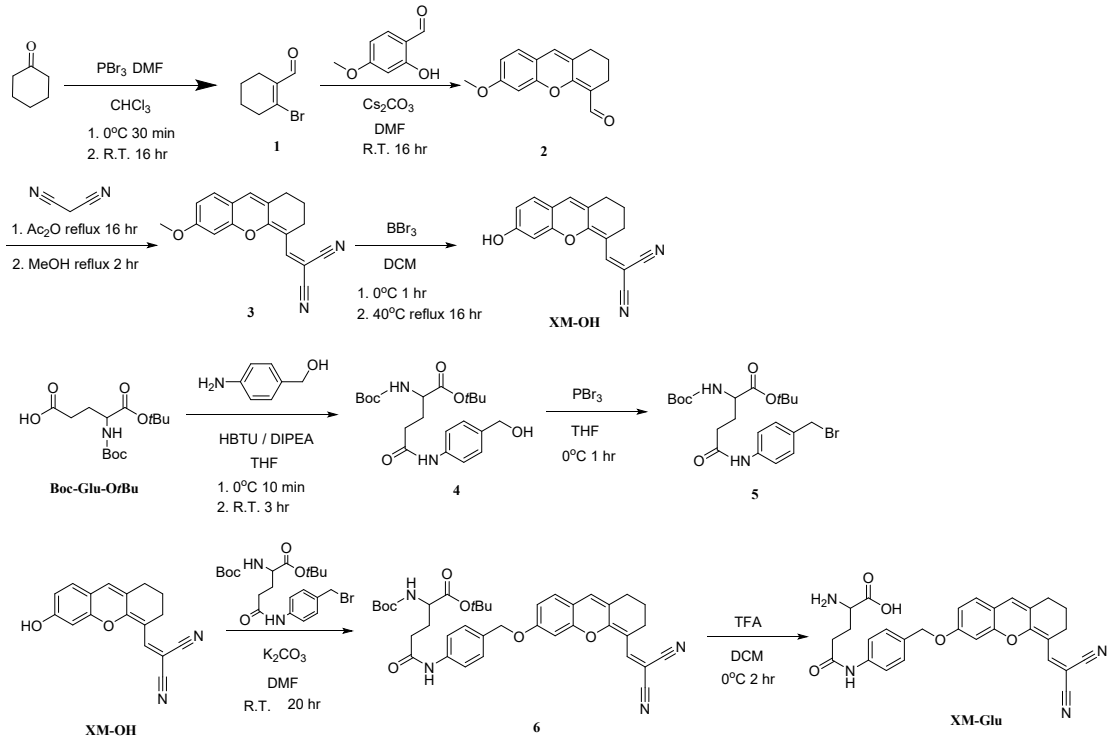

Scheme S1 Synthetic route of probe **XM-Glu**.

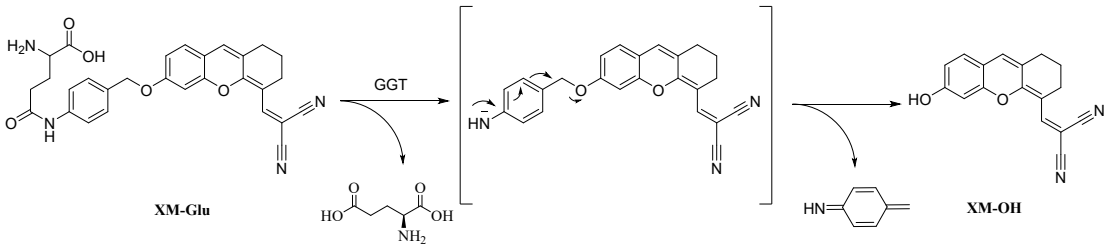

Scheme S2 Proposed reaction mechanism of **XM-Glu** reacted with GGT.

Synthesis of 2-bromocyclohex-1-ene-1-carbaldehyde (1)[1]

DMF (7.8 mL, 100 mmol) was mixed with 20 mL anhydrous chloroform. The reaction mixture was cooled to 0°C under N_2 condition. Then PBr_3 (3.8 mL, 40 mmol) was added dropwise to the solution, and it was stirred for 30 minutes. Cyclohexanone (2.06 mL, 20 mmol) was then added, and was reacted for another 16 hours at 25°C. After the reaction, the mixture was poured into ice H_2O and adjusted to pH 7 with solid $NaHCO_3$. The solution was extracted with DCM and H_2O. The organic layer was then dried over $MgSO_4$ and the solvent was removed to yield orange oil. The crude product was directly used in next step without further purification.^{1}H NMR (400 MHz, $CDCl_3$) δ 9.90 (s, 1H), 2.65 (m, 2H), 2.17 (m, 2H), 1.67 (m, 2H), 1.59 (m, 2H). ^{13}C NMR(100MHz, $CDCl_3$) δ 194.0, 144.0, 135.4, 38.5, 24.6, 23.9, 20.7.

Synthesis of 6-methoxy-2,3-dihydro-1*H*-xanthene-4-carbaldehyde (2)[1]

Compound **1** (1 g, 5.32 mmol), 2-hydroxy-4-methoxybenzaldehyde (402 mg, 2.64 mmol) and cesium carbonate (5 g, 15.35 mmol) were dissolved in 10 mL anhydrous DMF. The reaction mixture was stirred for 16 hours at room temperature. After the reaction, the mixture was filtered and the filtrate was extracted with DCM and H_2O for three times. The organic layer was then dried over $MgSO_4$ and the solvent was removed. The crude product was purified with column chromatography (Hexane/EtOAc = 4:1) to obtain compound **2** as a yellow solid (210 mg, 32%). ^{1}H NMR (400 MHz, $CDCl_3$) δ 10.32 (s, 1H), 7.08 (d, J = 9.2 Hz, 1H), 6.67-6.63 (m, 3H), 3.84 (s, 3H), 2.57 (t, J = 5.96 Hz, 2H), 2.45 (t, J = 6.08 Hz, 2H), 1.72 (tt, J_1= 6.16 Hz, J_2 = 5.96 Hz, 2H). ^{13}C

NMR (100 MHz) δ187.6, 161.4, 160.8, 153.4, 127.4, 126.8, 126.6, 114.6, 112.6, 110.9, 100.5, 55.6, 29.9, 21.5, 20.4. LRMS m/z (FD) calcd. for $C_{15}H_{14}O_3$: 242.1; found for: 242.1.

Synthesis of 2-((6-methoxy-2,3-dihydro-1*H*-xanthen-4-yl)methylene)malononitrile (3)[2]

Compound **2** (100 mg, 0.41 mmol) and malononitrile (41 mg, 0.62 mmol) were dissolved in 10 mL acetic anhydride. And the reaction mixture was refluxed under N_2 condition for 16 hours. After the reaction, 20 mL methanol was added and the reaction was refluxed for another 2 hr. The reaction mixture was concentrated, which was then purified by column chromatography with Hexane/EtOAc 3:1 (v/v) as the eluent to obtain compound **3** as a deep red solid (80 mg, 67%).^{1}H NMR (400 MHz, $CDCl_3$) δ 8.06 (s, 1H), 7.18 (d, J = 8.3 Hz, 1H), 6.90 (s, 1H), 6.80 – 6.75 (m, 2H), 3.89 (s, 3H), 2.87 (t, J = 6.0 Hz, 2H), 2.61 (t, J = 5.76 Hz, 2H), 1.83 (tt, J_1= 6.0 Hz, J_2 = 5.76 Hz, 2H). ^{13}C (100 MHz) δ 162.3, 158.6, 154.0, 150.3, 130.8, 127.9, 126.1, 117.6, 115.7, 114.8, 112.9, 109.8, 100.1, 70.2, 55.8, 29.1, 24.7, 20.5. MS m/z (FD) calcd. for $C_{18}H_{14}N_2O_2$: 290.1; found for: 290.1.

Synthesis of 2-((6-hydroxy-2,3-dihydro-1*H*-xanthen-4-yl)methylene)malononitrile (XM-OH)[2]

Compound **3** (252 mg, 0.87 mmol) was dissolved in 30 mL ultra-dry DCM, and BBr_3 (1.7 mL, 17.37 mmol) was added at 0°C under N_2 condition. The reaction mixture was stirred at 0°C for 1 hour and refluxed for another 16 hours. After the reaction, the reaction mixture was neutralized by saturated $NaHCO_3$ solution at 0°C, which was extracted with DCM and H_2O. The organic layer was then dried over $MgSO_4$ and the solvent was evaporated. The crude product was purified by column chromatography with Hexane/EtOAc 2:1 (v/v) as the eluent to obtain **XM-OH** as a deep red solid (144 mg, 60%).^{1}H NMR (400 MHz, DMSO-d_6) δ 10.6 (s, 1H), 8.15 (s, 1H), 7.37 (d, J = 8.44

Hz, 1H), 7.34 (s, 1H), 6.91 (d, J = 2.04 Hz, 1H), 6.75 (dd, J_1 = 8.44 Hz, J_2 = 2.04 Hz, 1H), 2.73 (t, J = 6.0 Hz, 2H), 2.60 (t, J = 5.76 Hz, 2H), 1.74 (tt, J_1 = 6.0 Hz, J_2 = 5.76 Hz, 2H). ^{13}C NMR (150 MHz, DMSO-d_6) 116.89, 114.25, 114.03, 109.33, 102.67, 66.65, 28.46, 24.77, 20.51 LRMS m/z (FD) calcd. for $C_{17}H_{12}N_2O_2$: 276.1; found for: 276.1.

Synthesis of tert-butyl N^2-(tert-butoxycarbonyl)-N^5-(4-(hydroxymethyl)phenyl)glutaminate (4)[3]

N-(tert-butoxycarbonyl)glutamic acid tert-butyl ester (**Boc-Glu-O*t*Bu**) (455 mg, 1.5 mmol), hexafluorophosphate benzotriazole tetramethyl uranium (HBTU) (569 mg, 1.5 mmol) and *N,N*-diisopropylethylamine (DIPEA) (412 µL, 3 mmol) were added to anhydrous THF (8 mL) and stirred for 30 minutes. Then the reaction mixture was treated with *p*-aminobenzeyl alcohol (222 mg, 1.8 mmol) and stirred at 0°C for 10 minutes and then at room temperature for 3 hours. After the reaction, the solvent was removed under reduced pressure. The reaction mixture was extracted with EtOAc and brines. The organic layer was then dried over $MgSO_4$ and the solvent was evaporated. The crude product was purified by column chromatography with Hexane/EtOAc 1:1 (v/v) as the eluent to obtain compound **4** as a light yellow solid (560 mg, 91%).^{1}H NMR (400 MHz, $CDCl_3$) (**Figure S22**) δ 8.84 (s, 1H), 7.60 (d, J = 8.12 Hz, 2H), 7.32 (d, J = 8.12 Hz, 2H), 5.36 (d, J = 7.60 Hz 1H), 4.64 (d, J = 4.00 Hz 2H), 4.22 (m, 1H), 2.43 (m, 2H), 2.26 (m, 2H), 1.46 (s, 18H) ^{13}C NMR (100 MHz, $CDCl_3$) (**Figure S23**) δ 171.24, 170.58, 156.56, 137.88, 136.50, 127.75, 119.83, 82.75, 80.51, 65.01, 5 3.20, 34.14, 30.68, 28.30, 27.96 LRMS m/z (FD) (**Figure S24**) calcd. for $C_{21}H_{32}N_2O_6$: 408.2; found for: 408.2.

Synthesis of *tert*-butyl N^5-(4-(bromomethyl)phenyl)-N^2-(tert-butoxycarbonyl)glutaminate (5)[3]

Compound **4** (244 mg, 0.6 mmol) was dissolved in anhydrous THF (10 mL), and

PBr_3 (57 μL, 0.6 mmol) was added at 0°C under N_2 condition. The reaction mixture was stirred at 0°C for 1 hours. Then, the reaction mixture was added to a saturated $NaHCO_3$ solution (20 mL) at 0°C, which was then extracted with EtOAc and H_2O. The organic layer was then dried over $MgSO_4$ and the solvent was evaporated. The crude product was used in next step without further purification. (172 mg, 61%).

Preparation of stock solution

Solutions of cysteine, homocysteine, glutathione, hydrogen peroxide, and HOCl were prepared in distilled water at a concentration of 1 mM. Enzymes including acetylcholinesterase, alkaline phosphatase, b-galactosidase, g-glutamyl transpeptidase, and tyrosinase were produced at 1U/mL in 10 mM PBS buffer. Singlet oxygen was created by combining 1 mM hydrogen peroxide with sodium hypochlorite, while O2- was created by dissolving 1 mM potassium superoxide in distilled water. Solutions with pH ranging from 4.0 to 12.0 were prepared in a 10 mM PBS buffer by adding various concentrations of 1M HCl or 1M NaOH. For photophysical studies, a solution of **XM-Glu** (20 μM) was prepared by diluting the stock solution in a mixture of H_2O and DMSO (volume ratio of 6:4) with 6 mM PBS buffer (pH 7.4).

Cytotoxicity test

The cytotoxicity of the probe **XM-Glu** probe was evaluated using MTT tests. HepG2 and HEK293 cells were planted on 96 well plates with 200 L Dulbecco modified Eagle medium (DMEM) and incubated for 24 hours at 37°C under 5% CO_2. Various concentrations of XM-Glu (0, 5, 10, 15, and 25 μM) were incubated with the cells for an additional 24 hours. The cells were treated with 1 mg/mL of 3-(4,5-dimethylthiazol-2-yl)-2,5-diphenyltetrazolium bromide (MTT) for 4 hours, and then the purple crystals were dissolved in DMSO. The absorbance (570 nm) was measured by microplate readers. The following equation shows the calculation for cell viability:

$$Cell\ viability\ (\%) = \frac{average\ absorbance\ of\ treatment\ group}{average\ absorbance\ of\ control\ group} \times 100\%$$

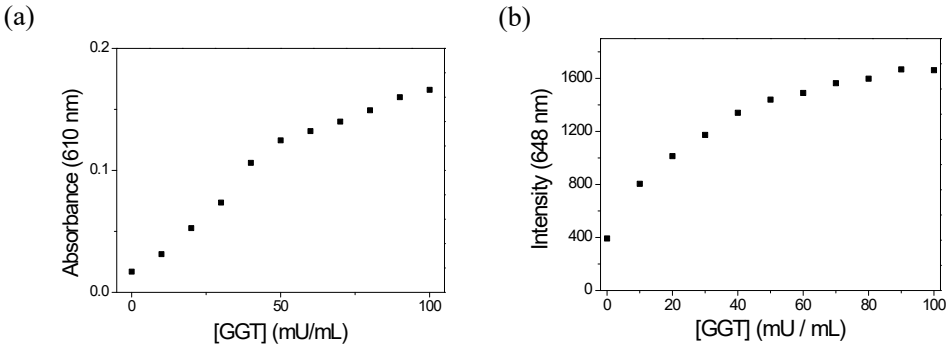

Figure S1 (a) Absorbance changes at 610 nm and (b) fluorescence changes at 648 nm of **XM-Glu** (20 μM) in response to various concentration of GGT (0-100 mU/mL) in DMSO-H_2O (v/v = 4/6, 6 mM PBS buffer, pH 7.4) solution for 4 h. λ_{ex} = 595 nm.

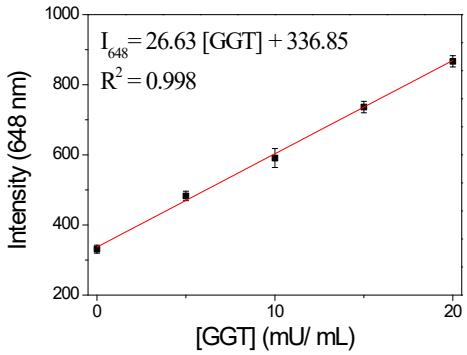

Figure S2 The fluorescence intensity at 648 nm of the probe **XM-Glu** (20 μM) in response to GGT (0-20 mU/mL) in DMSO-H_2O (v/v = 4/6, 6 mM PBS, pH 7.4) solution for 4 h. (λ_{ex} = 595 nm) The detection limit was calculated to be 0.067 mU/mL.

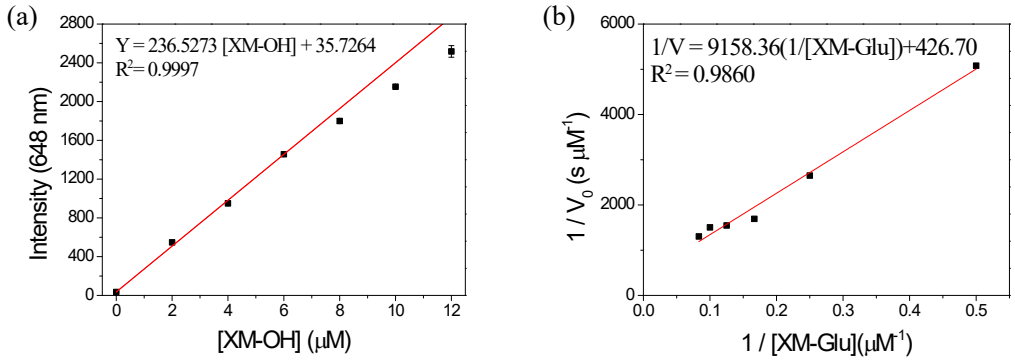

Figure S3 (a) The fluorescence intensity at 648 nm of fluorophore **XM-OH** (0 ~ 12 μM) in DMSO- H_2O (v/v = 4/6, 6 mM PBS, pH 7.4) solution. (b) Lineweaver-Burk plot of probe **XM-Glu** in response to GGT (100 mU/mL). λ_{ex}= 595 nm

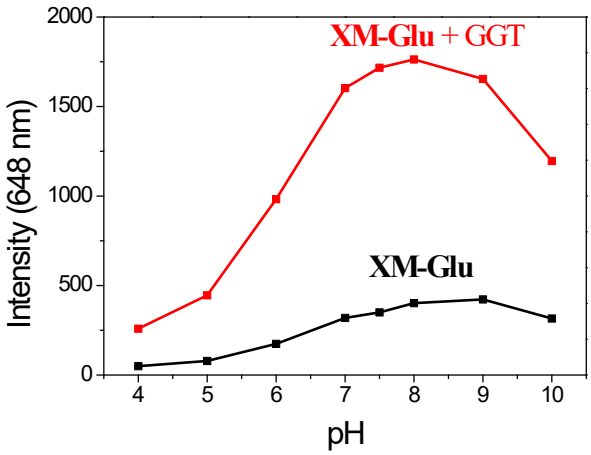

Figure S4 The fluorescence changes of **XM-Glu** (20 μM), and **XM-Glu** (20 μM) with GGT (100 mU/mL) in different pH value of DMSO-H_2O (v/v = 4/6, 6 mM PBS) solution for 4 h. λ_{ex} = 595 nm.

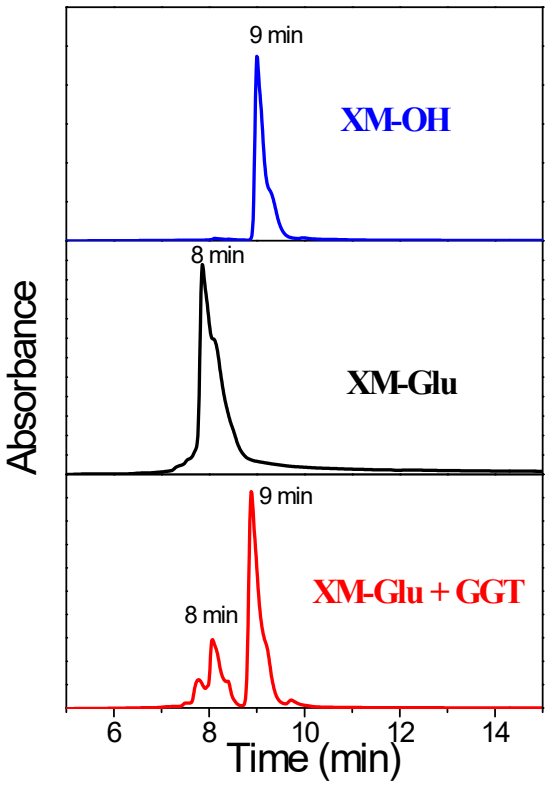

Figure S5 HPLC chromatograms of fluorophore **XM-OH** (100 μM), probe **XM-Glu** (100 μM), and **XM-Glu** (100 μM) + GGT (400 mU/mL). The absorption peak was measured at 520 nm. (HPLC conditions: 0 min: 80% H_2O + 20% MeOH, 5 ~ 15 min: 4.5 % H_2O + 95.5% MeOH, 20 min: 100% MeOH)

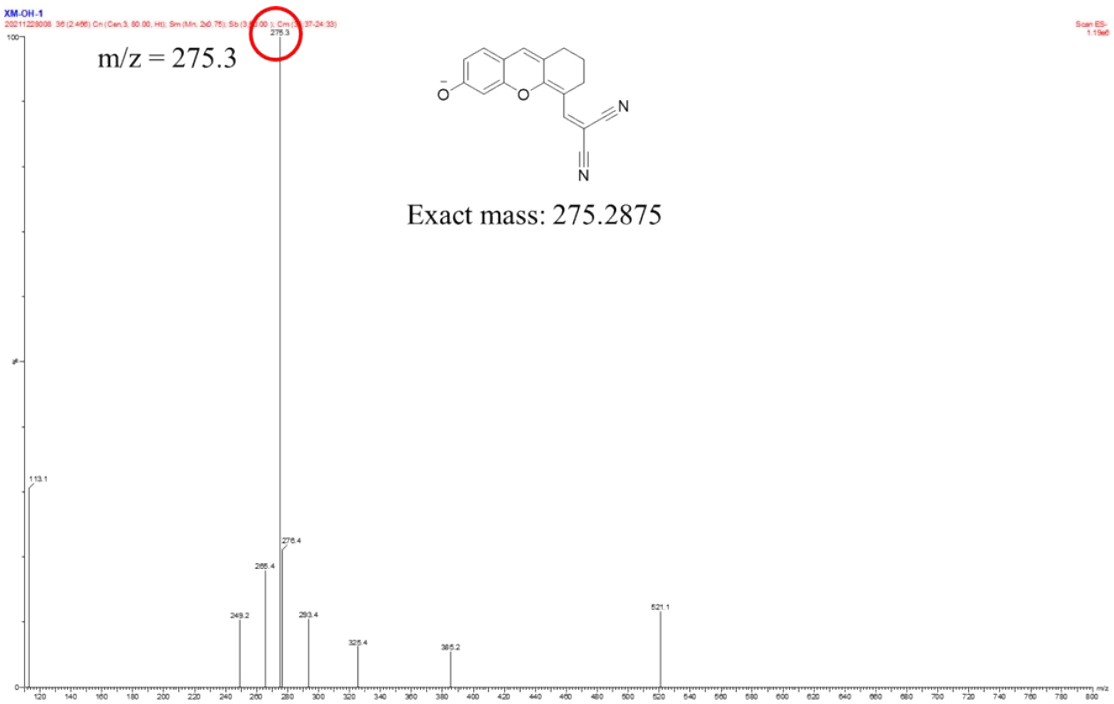

Figure S6 ESI-MS spectra of **XM-Glu** reacted with GGT.

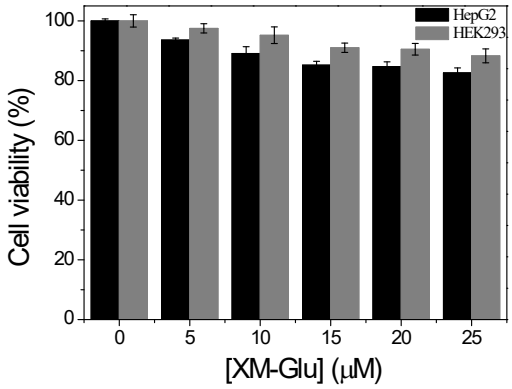

Figure S7 Cell viability of HepG2 and HEK293 cells treated with **XM-Glu** (0, 5, 10, 15, 20, 25 μM) at 37°C for 24 h. The results are the mean and standard deviation of three independent experiments.

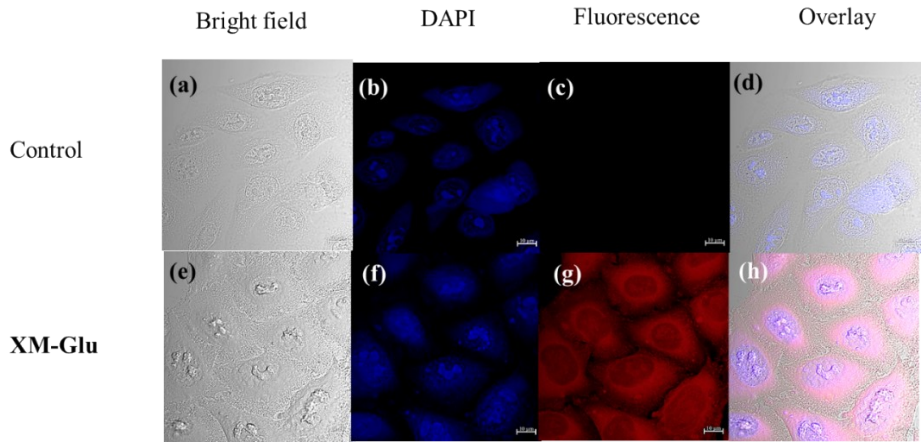

Figure S8 Fluorescence images of HeLa cells. (a ~ d) Control group. (e ~ h) HeLa cells were incubated with **XM-Glu** (10 μM) at 37°C for 2 h (Blue fluorescence: λ_{ex} = 405 nm. λ_{em} = 435 ~ 485 nm. Red fluorescence: λ_{ex} = 561 nm. λ_{em} = 600 ~ 700 nm).

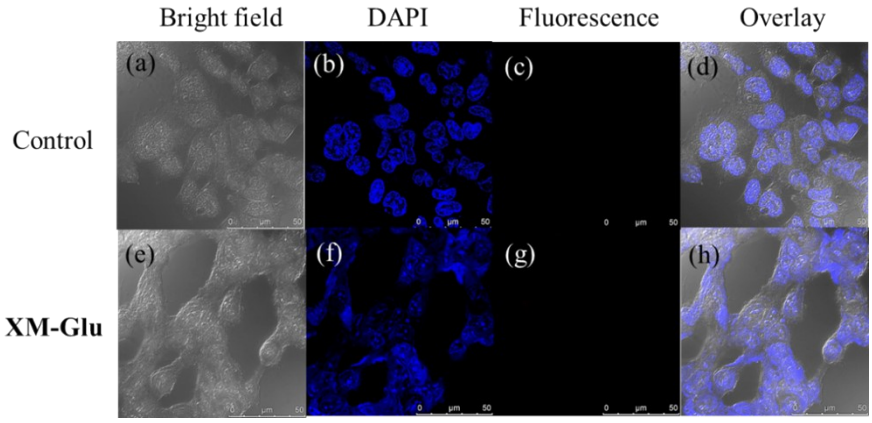

Figure S9 Fluorescence images of HEK293 cells. Control group (a–d). Experimental group treated with **XM-Glu** (10 μM) at 37°C for 2 hours (e–h). DAPI fluorescence: Excitation wavelength = 405 nm, Emission wavelength = 435–485 nm. Red fluorescence: Excitation wavelength = 561 nm, Emission wavelength = 600–700 nm.

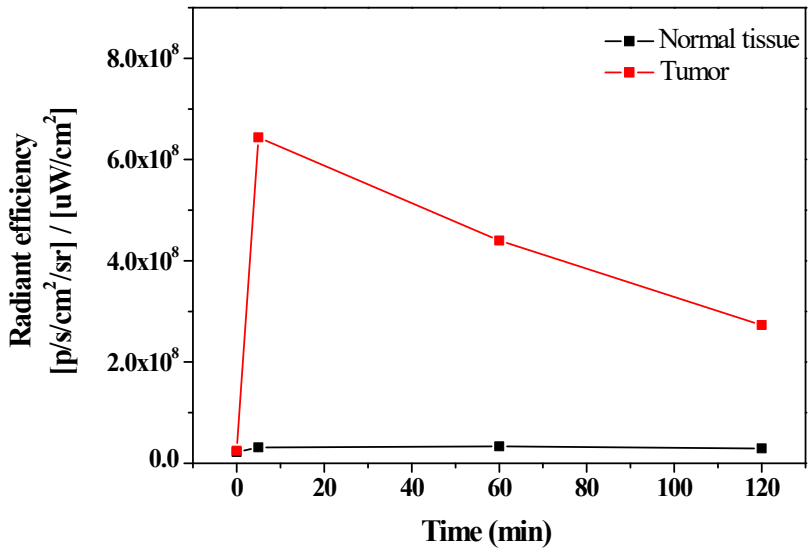

Figure S10 Fluorescence intensity at tumor site pre-injection, 5 min after injection, 1 h after injection, and 2 h after injection.

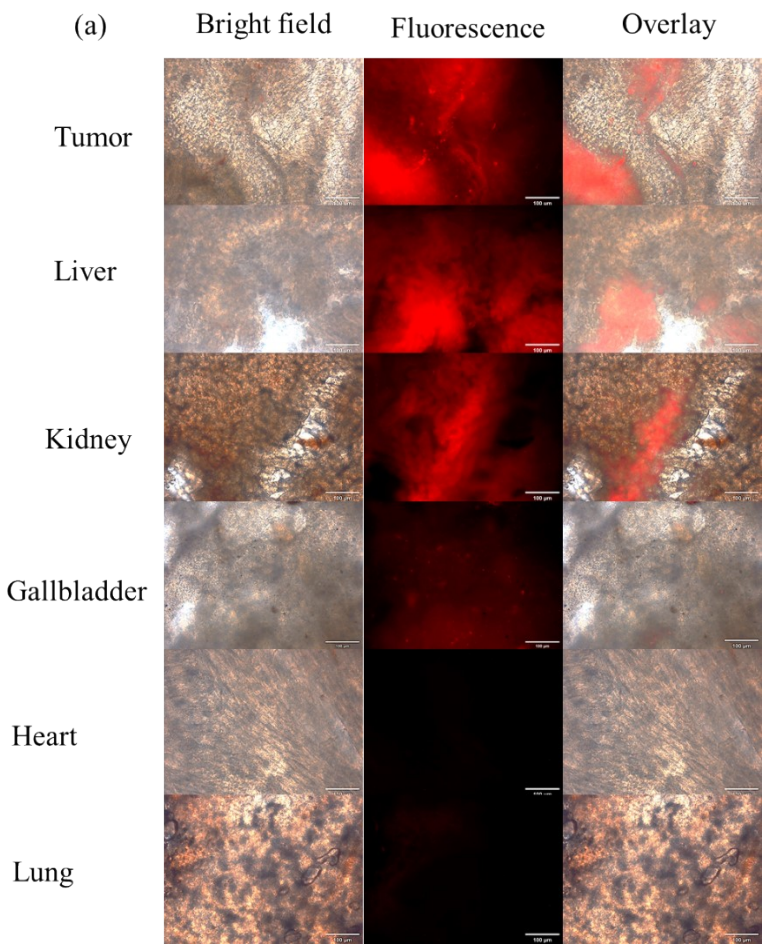

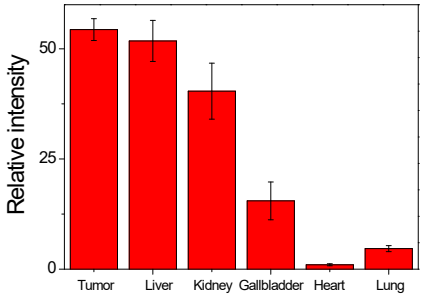

Figure S11 (a) Fluorescence imaging of tissue sections from tumors and organs of mouse incubated with **XM-Glu** (50 μM) for 2 h. Fluorescence: λ_{ex} = 545 nm. λ_{em} = 590 ~ 650 nm. (b) Relative intensity plots of the images.

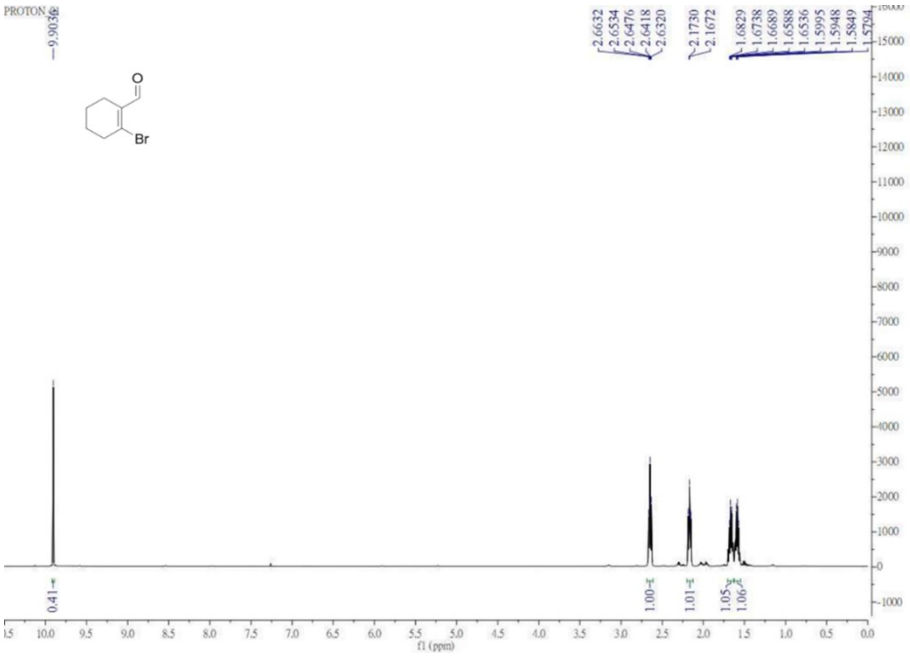

Figure S12 ^{1}H NMR (400 MHz) spectrum of Compound **1** in $CDCl_3$.

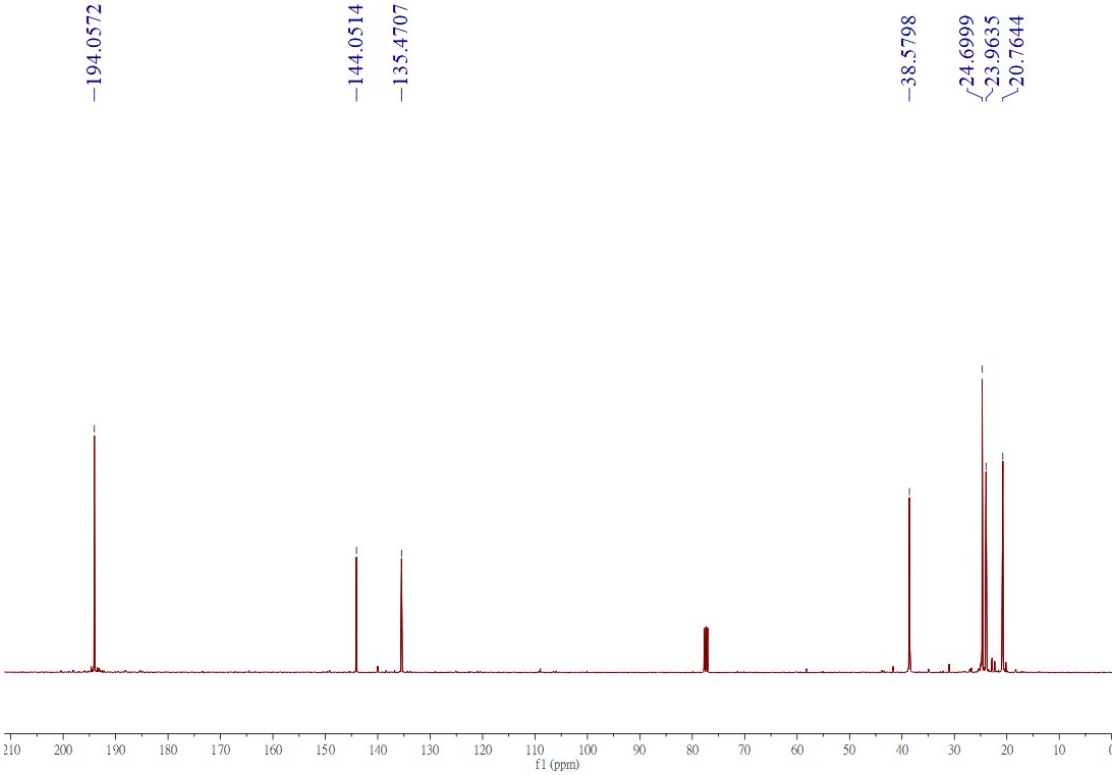

Figure S13 ^{13}C NMR (100 MHz) spectrum of Compound **1** in $CDCl_3$.

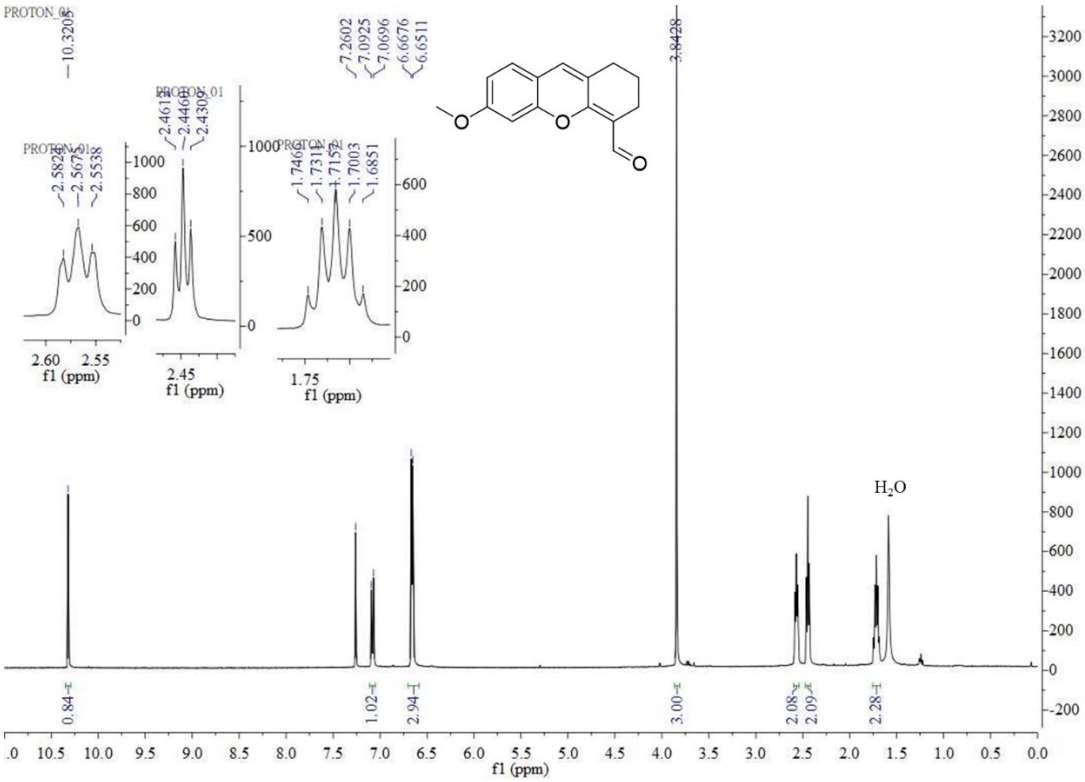

Figure S14 ^{1}H NMR (400 MHz) spectrum of Compound **2** in $CDCl_3$.

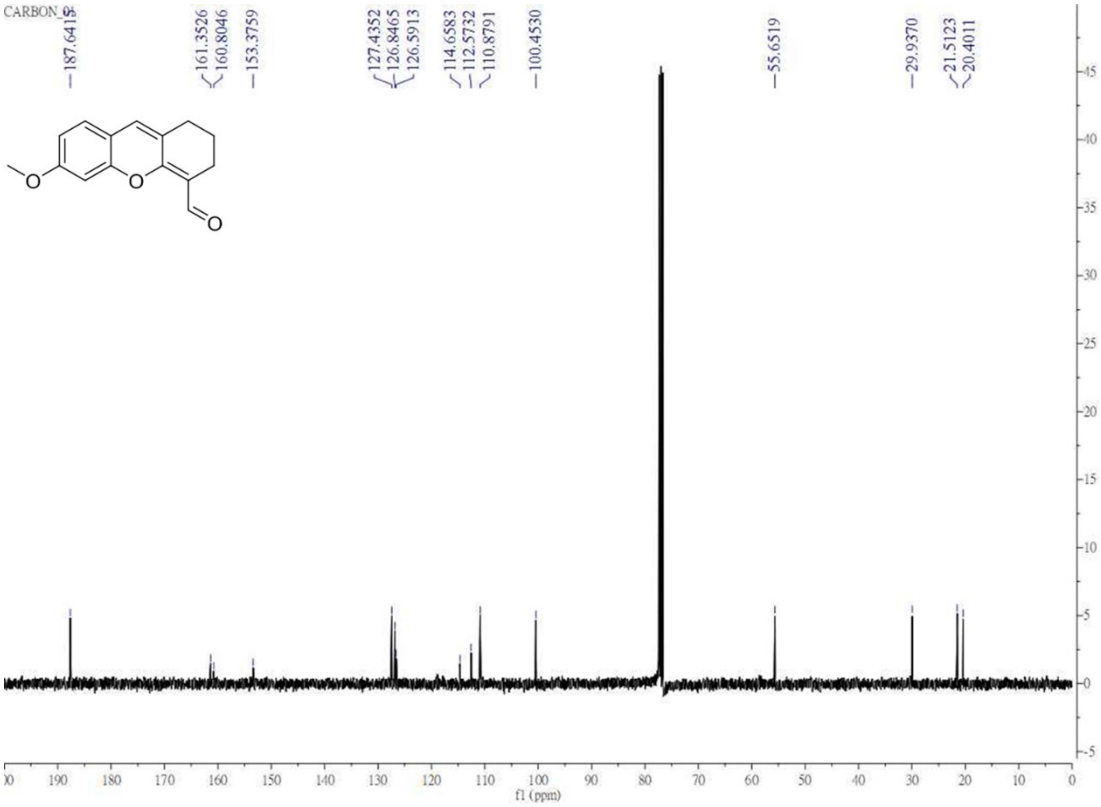

Figure S15 ^{13}C NMR (100 MHz) spectrum of Compound **2** in $CDCl_3$.

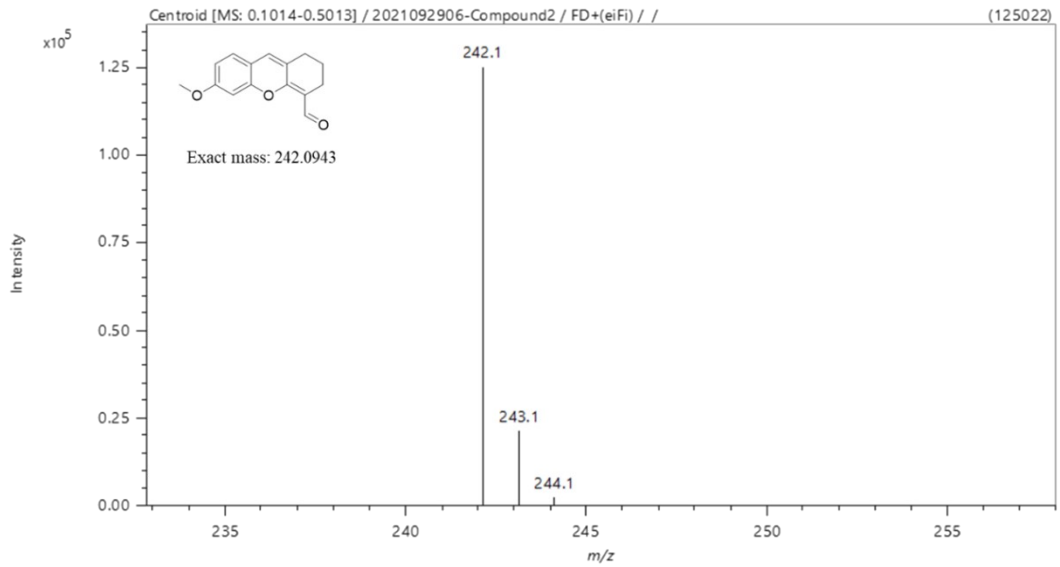

Figure S16 FD mass spectrum of compound **2**.

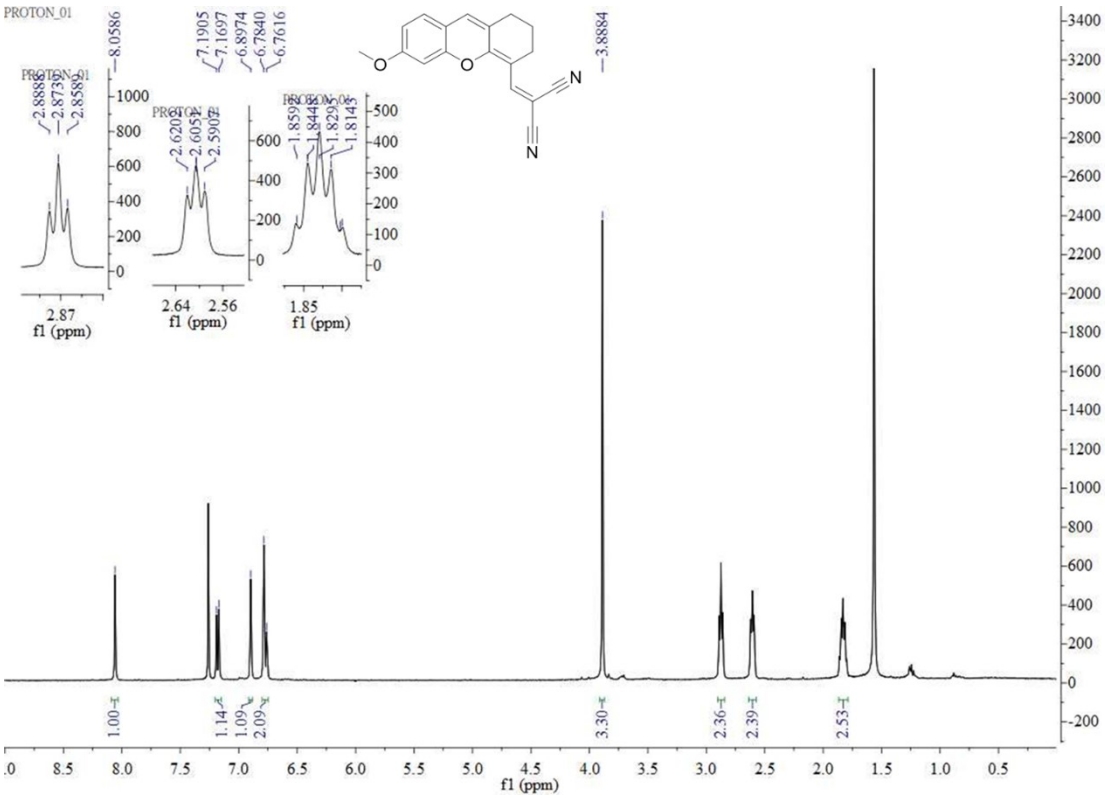

Figure S17 ^{1}H NMR (400 MHz) spectrum of Compound **3** in $CDCl_3$.

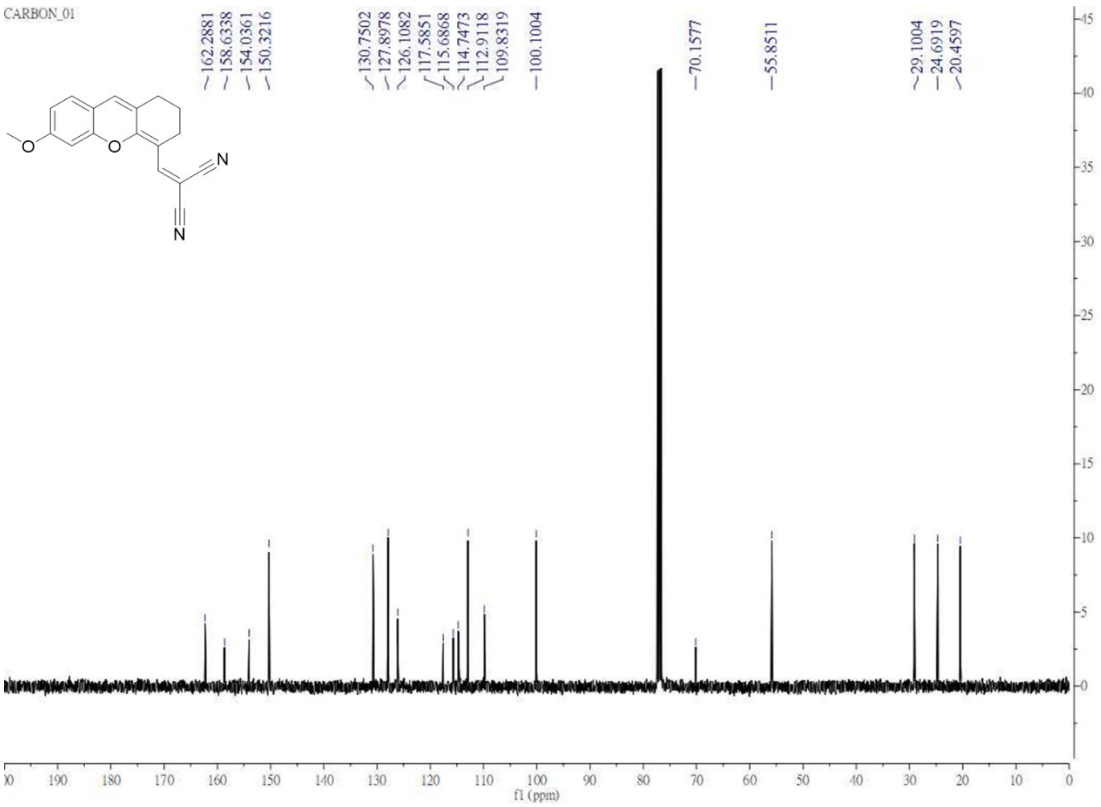

Figure S18 ^{13}C NMR (100 MHz) spectrum of Compound **3** in $CDCl_3$.

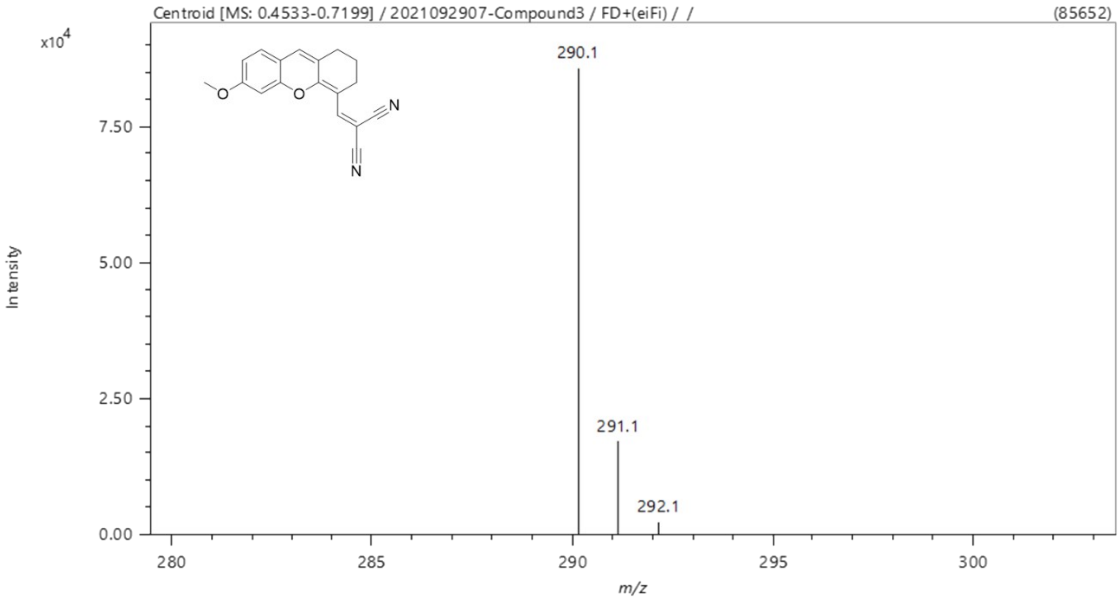

Figure S19 FD mass spectrum of compound **3**

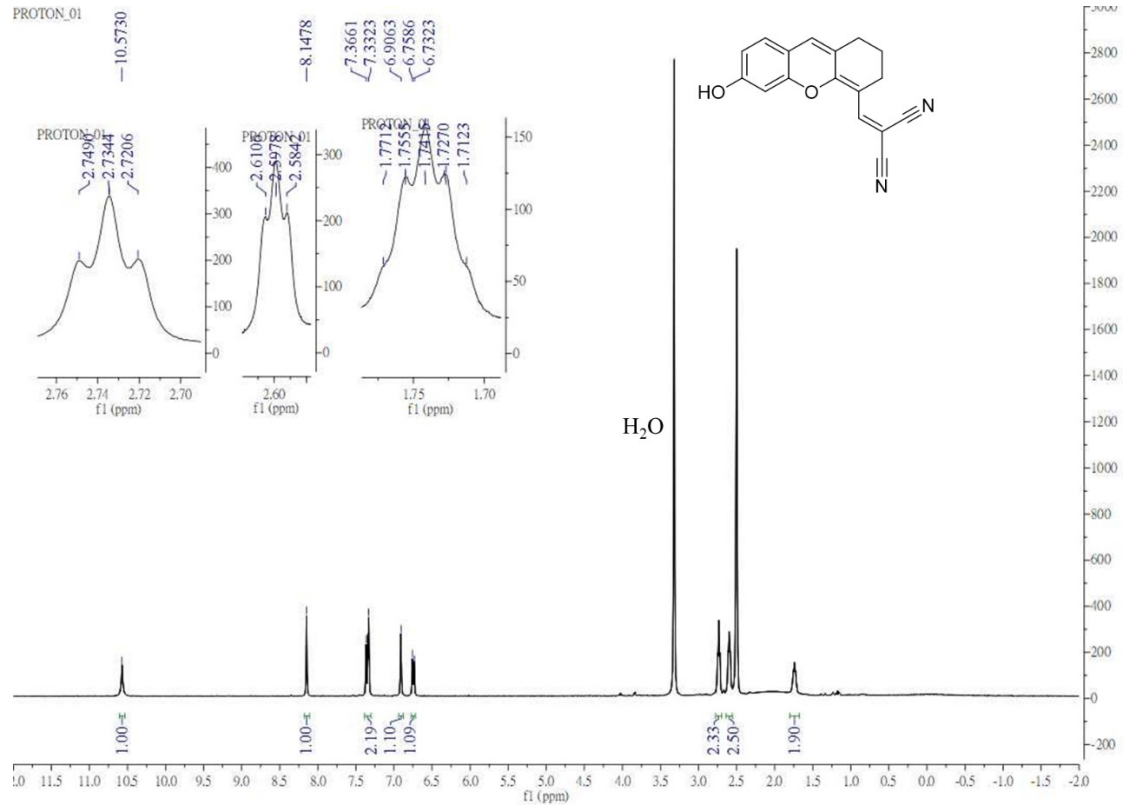

Figure S20 ^{1}H NMR (400 MHz) spectrum of **XM-OH** in DMSO-d_6.

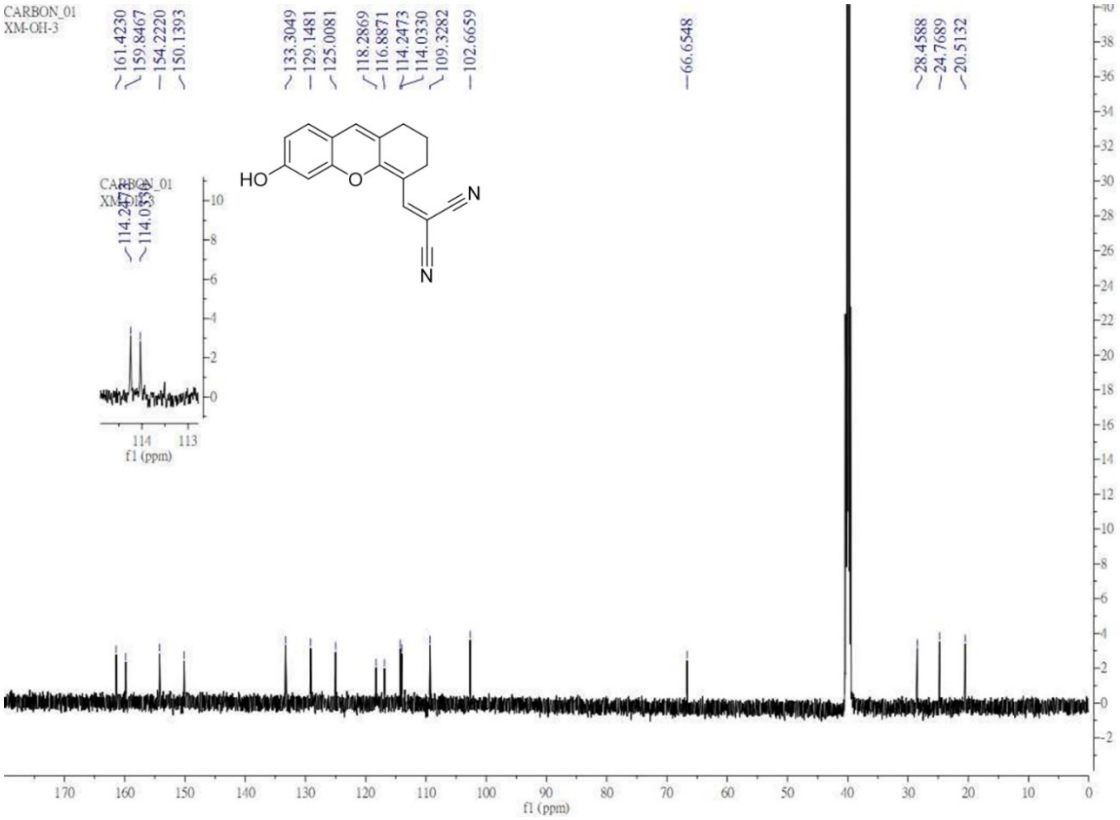

Figure S21 ^{13}C NMR (150 MHz) spectrum of **XM-OH** in DMSO-d_6.

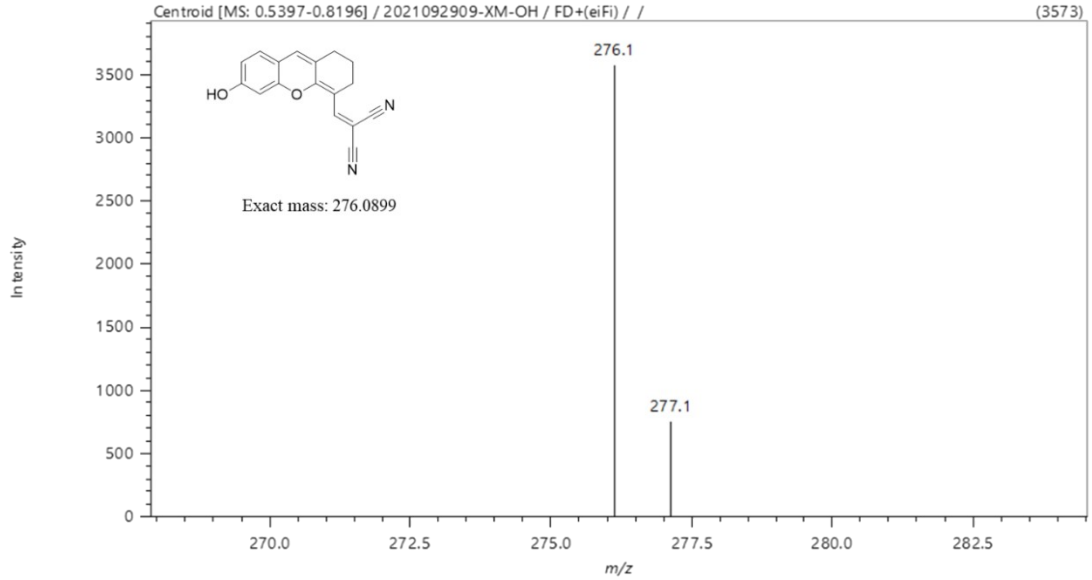

Figure S22 FD mass spectrum of **XM-OH**.

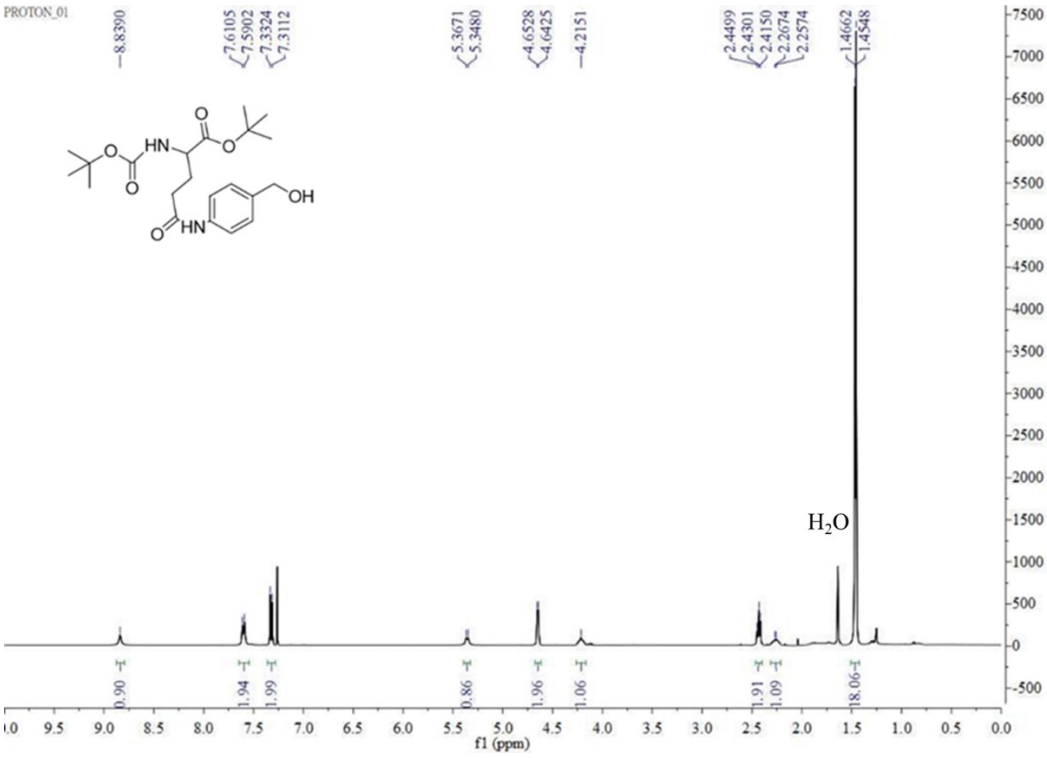

Figure S23 ^{1}H NMR (400 MHz) spectrum of Compound **4** in $CDCl_3$.

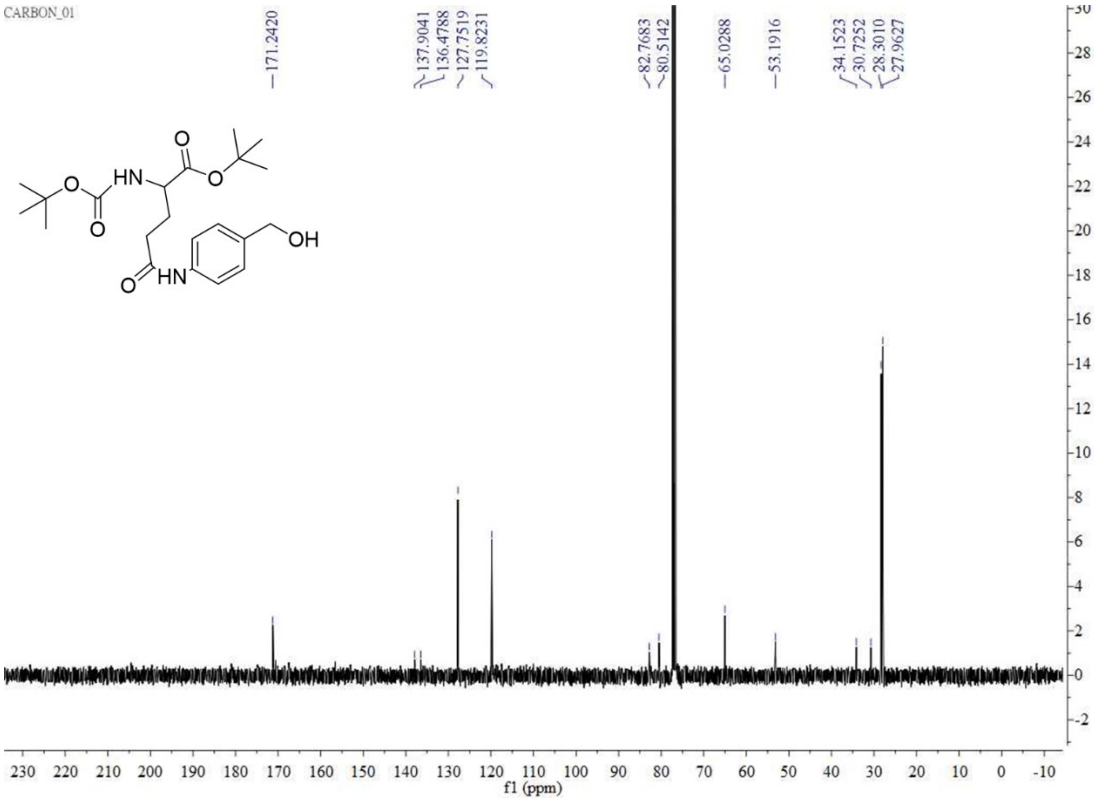

Figure S24 ^{13}C NMR (100 MHz) spectrum of Compound **4** in $CDCl_3$.

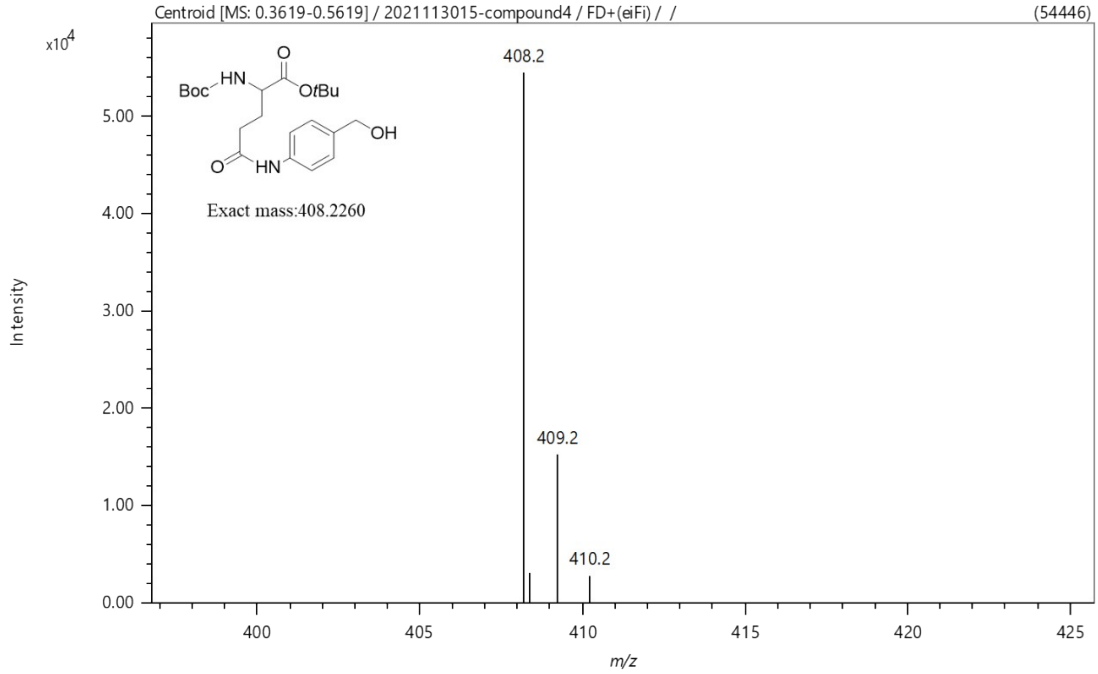

Figure S25 FD mass spectrum of compound **4**.

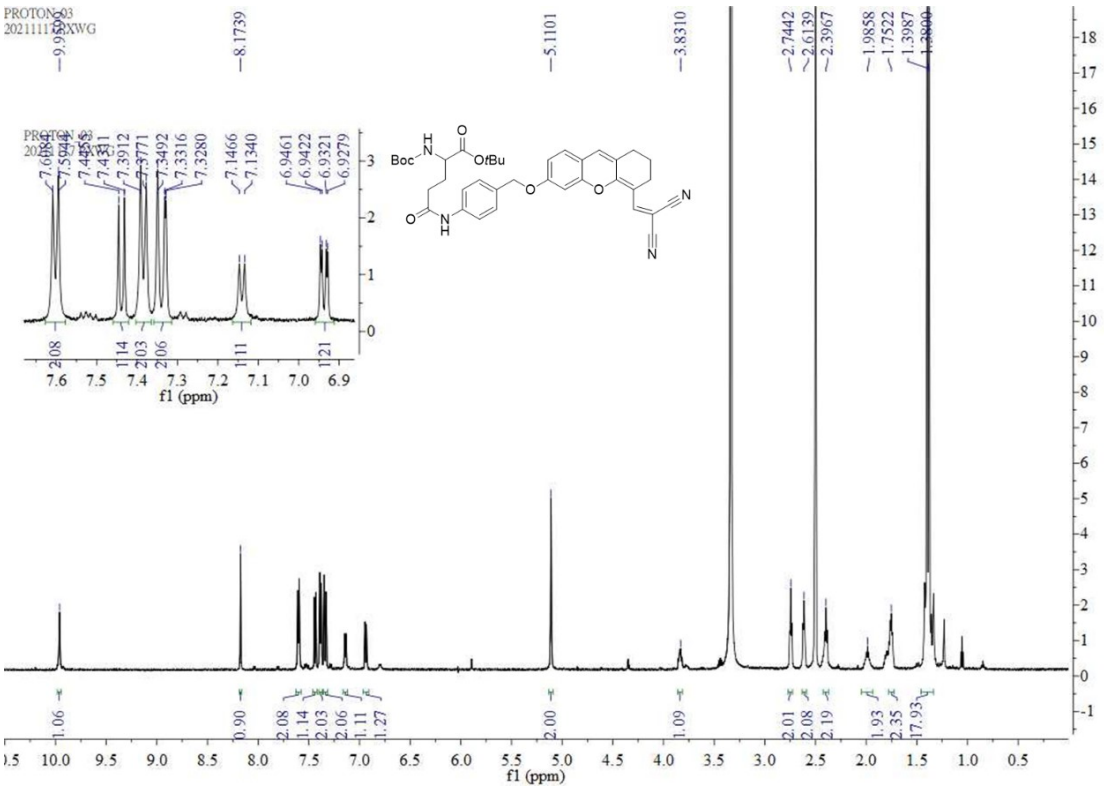

Figure S26 ^{1}H NMR (600 MHz) spectrum of Compound **6** in DMSO-d_6.

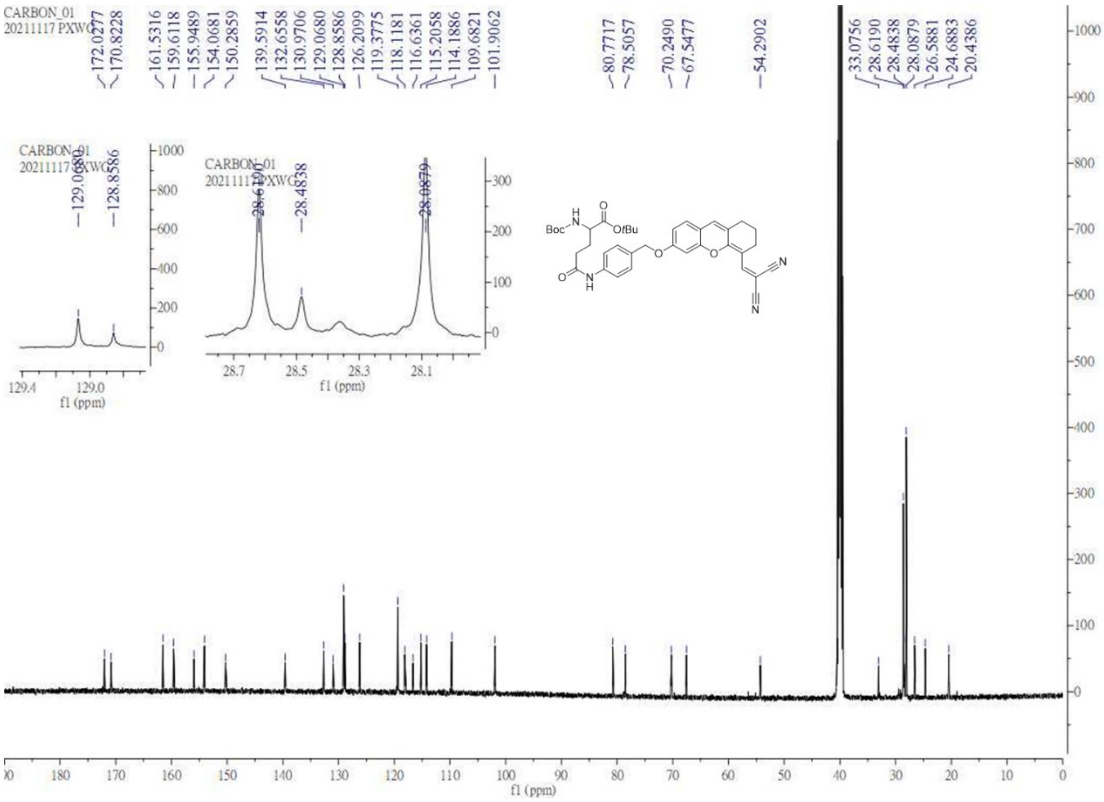

Figure S27 ^{13}C NMR (150 MHz) spectrum of Compound **6** in DMSO-d_6.

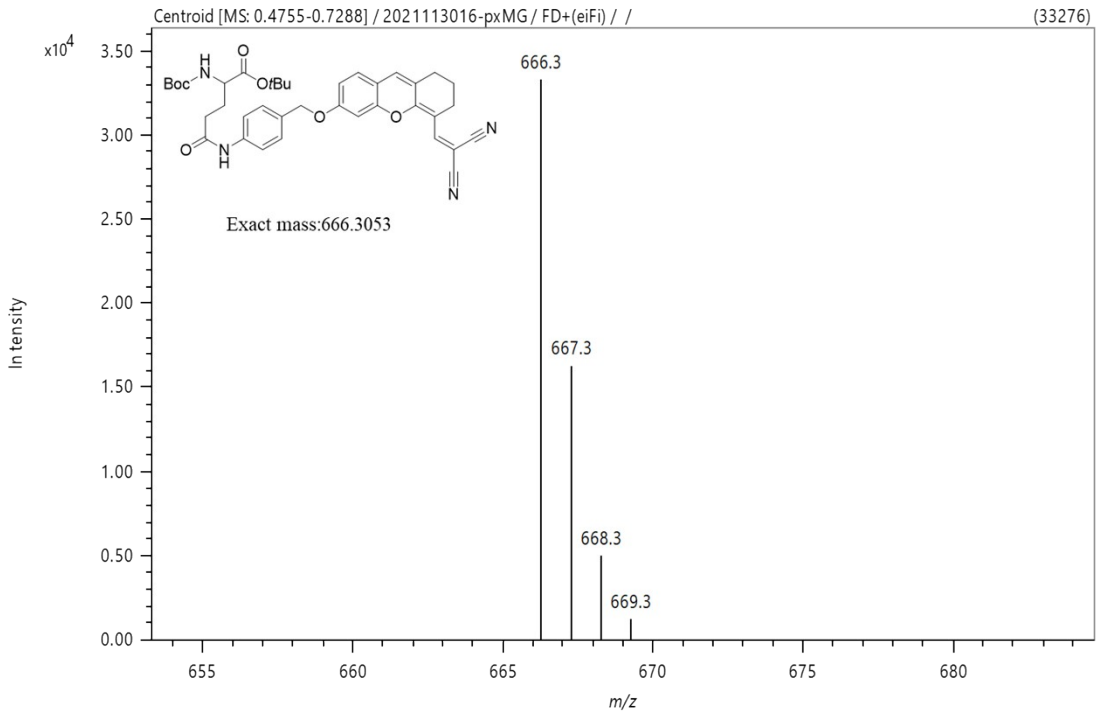

Figure S28 FD mass spectrum of compound **6**.

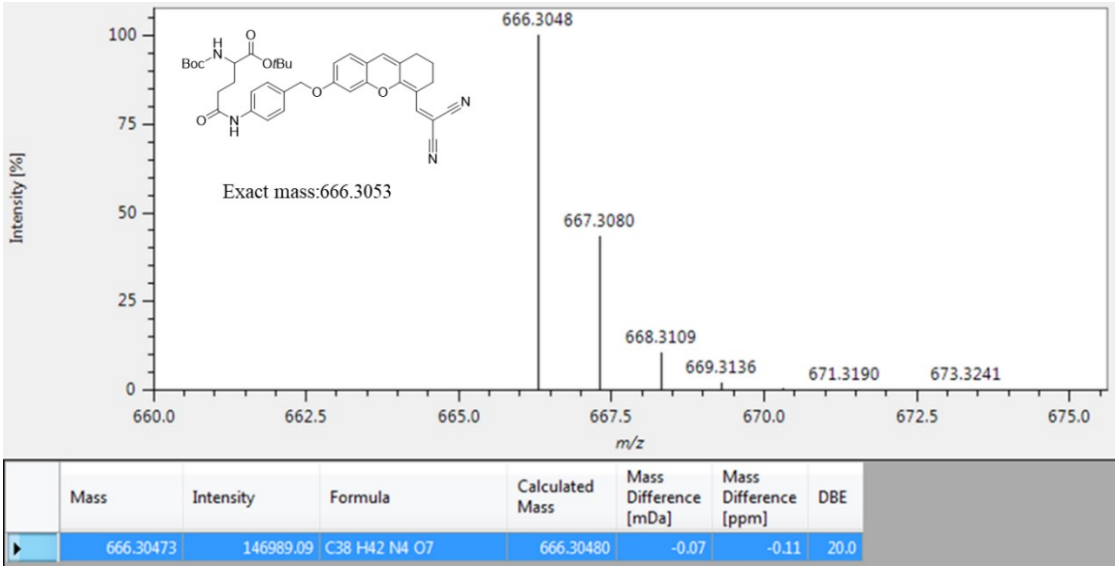

Mass	Intensity	Formula	Calculated Mass	Mass Difference [mDa]	Mass Difference [ppm]	DBE
666.30473	146989.09	C38 H42 N4 O7	666.30480	-0.07	-0.11	20.0

Figure S29 HR-FD mass spectrum of compound **6**.

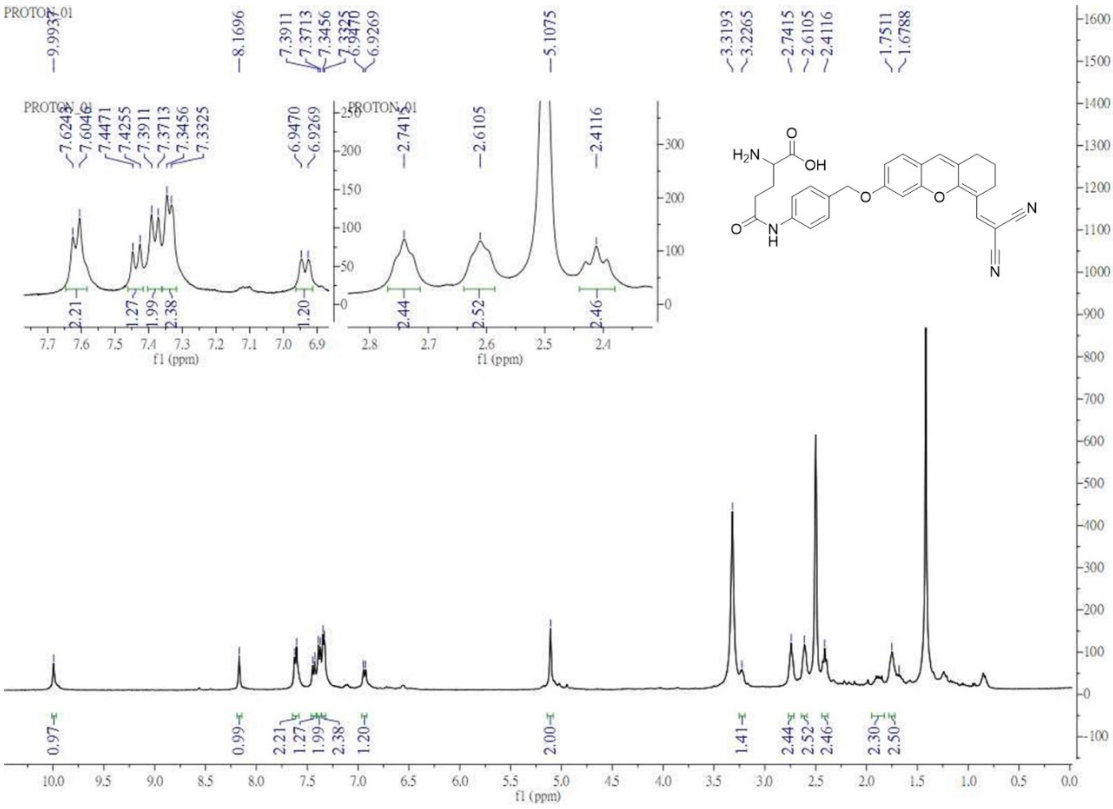

Figure S30 ^{1}H NMR (400 MHz) spectrum of **XM-Glu** in DMSO-d_6.

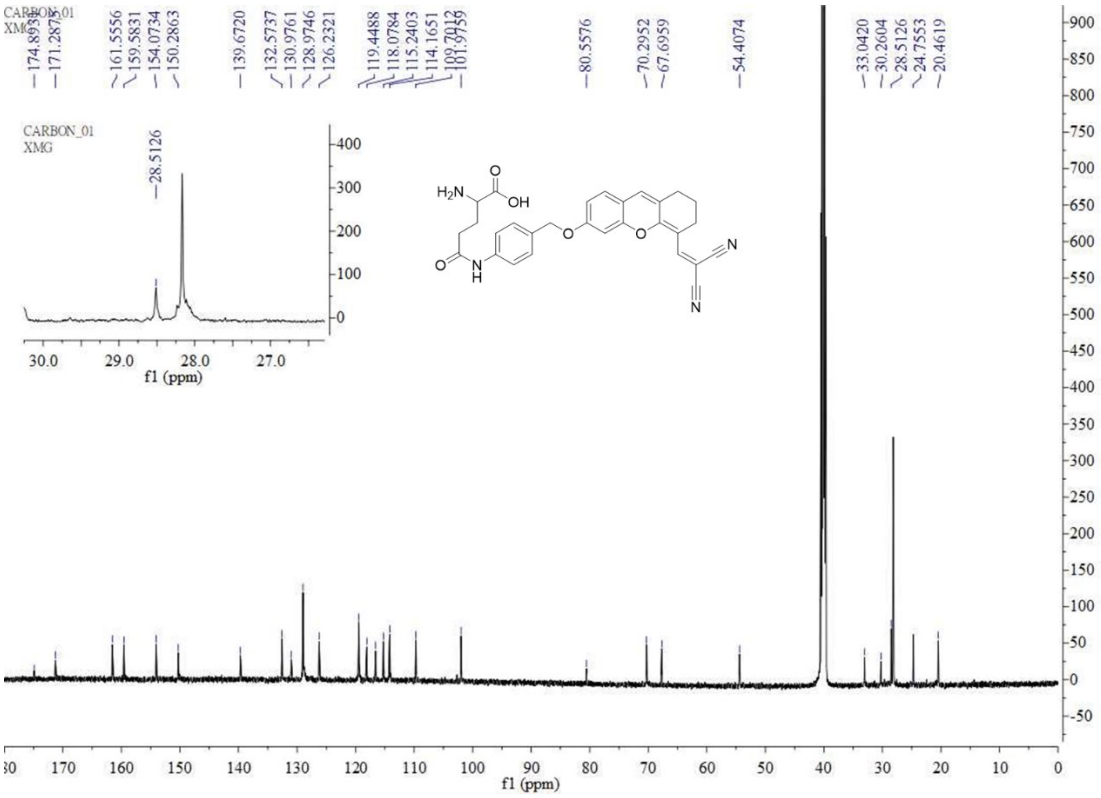

Figure S31 ^{13}C NMR (150 MHz) spectrum of **XM-Glu** in DMSO-d_6.

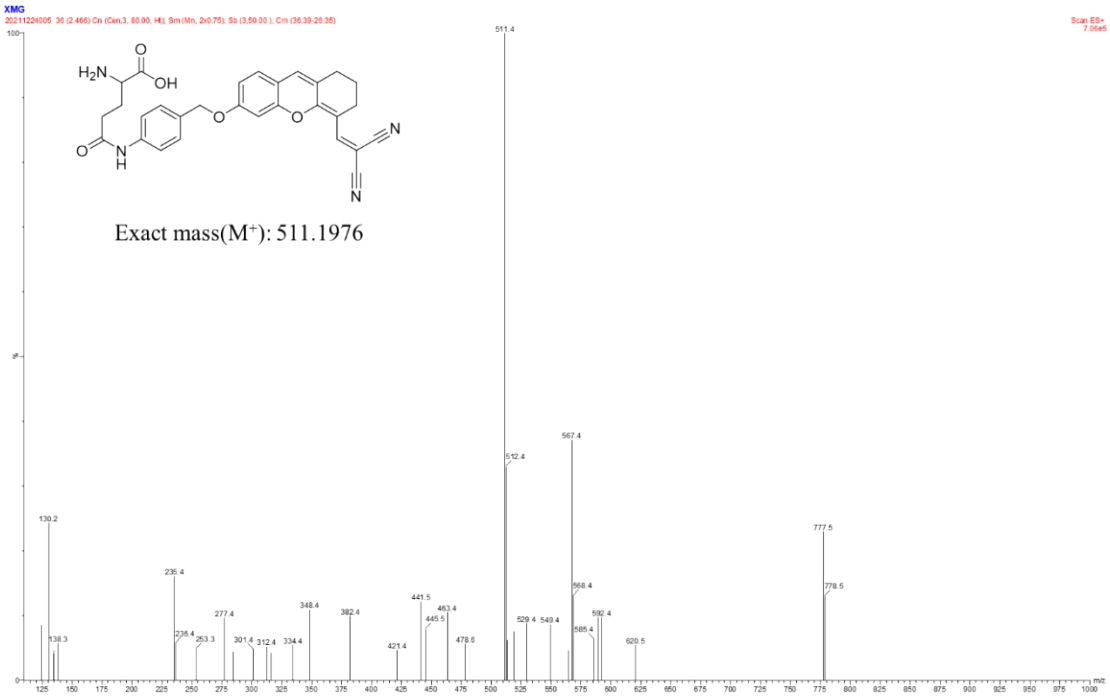

Figure S32 ESI mass spectrum of **XM-Glu**.

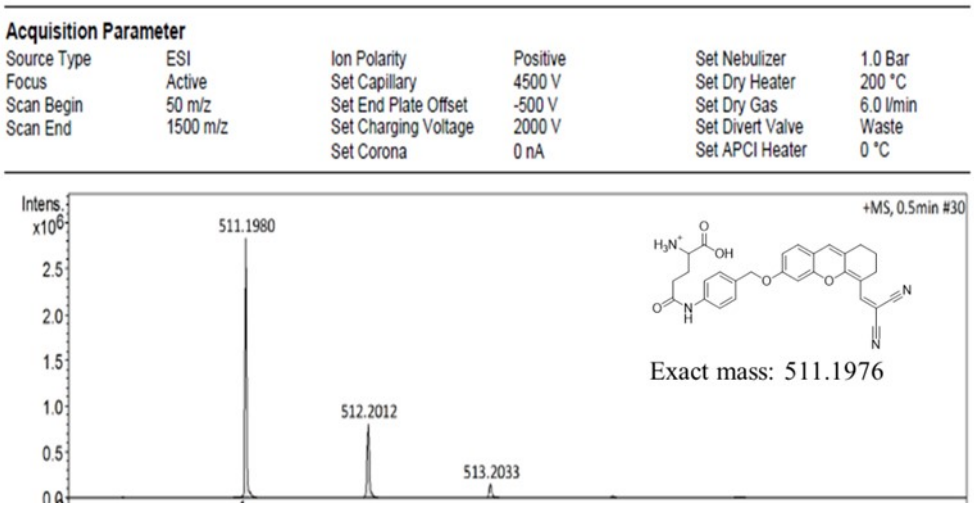

Figure S33 HR-ESI mass spectrum of **XM-Glu**.

Table S1 Published fluorescent probes for the detection of GGT.

Probe structure	**$\lambda_{ex}/\lambda_{em}$**	**Detection limit (mU / mL)**	**K_m (μM) V_{max} (μM s^{-1}) k_{cat} (s^{-1})**	**Ref.**
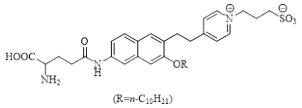	451 nm / 610 nm	1.47	N.D.	4

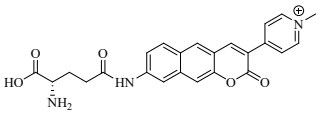	390 nm / 640 nm	2.27	K_m =19.3 k_{cat} = 0.118	5
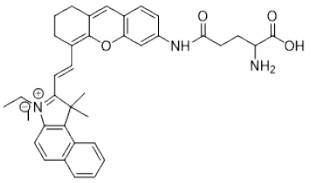	680 nm / 727 nm	0.4	K_m = 4.264 V_{max} = 0.04	6
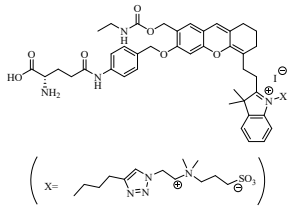	687 nm / 714 nm	N.D.	N.D.	7
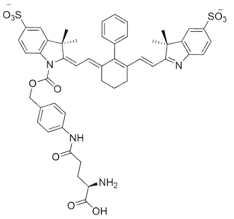	710 nm / 770 nm	N.D.	K_m = 16	8
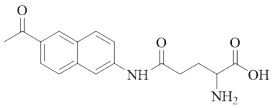	355 nm / 500 nm	0.3	K_m = 9.8	9
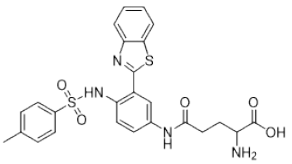	365 nm / 650 nm	2.9	K_m = 7.68	10
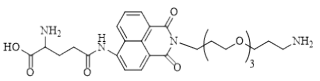	408 nm / 550 nm	0.76	N.D.	11
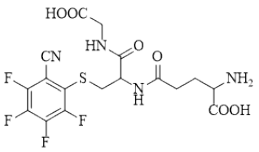	405 nm / 490 nm	0.117	N.D.	12
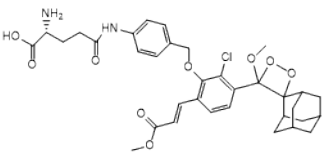	λ_{em}=540 nm (Chemiluminescence)	0.016	N.D.	13

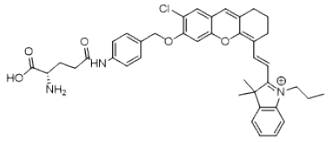	680 nm / 720 nm	0.0036	K_m =1.26 k_{cat} = 0.004	3
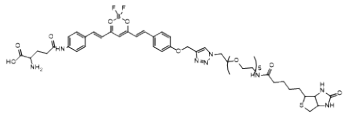	600 nm / 670 nm	0.0785	K_m =6.62 V_{max} =0.103	14
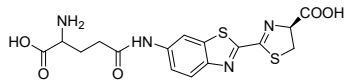	λ_{em}= 600 nm (Bioluminescence)	0.192	K_m =12.57 V_{max} =0.057 k_{cat} = 0.917	15
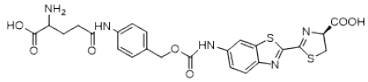	λ_{em}= 600 nm (Bioluminescence)	0.442	K_m = 18.42 V_{max} = 0.031 k_{cat} = 0.5	15
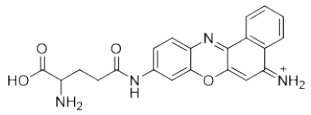	585 nm / 615 nm	0.0056	K_m =7.64	16
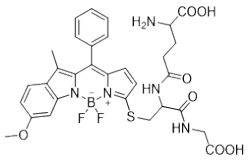	578 nm / 601 nm	N.D.	K_m =18.7 V_{max} = 0.06	17
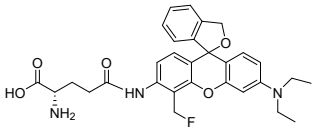	530 nm / 565 nm	N.D.	N.D.	18
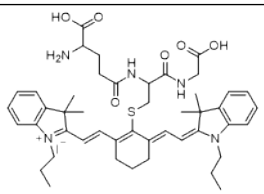	540 nm / 640 nm	0.03	K_m = 9.87 V_{max} = 0.021	19
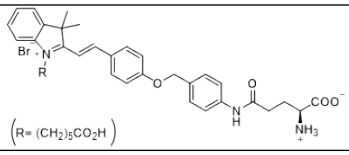	460 nm / 557 nm	0.15	N.D.	20
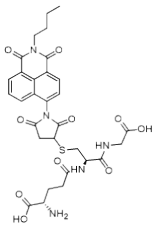	354 nm / 473 nm	0.21	K_m =17.64 V_{max} = 0.024	21

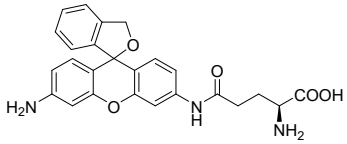	496 nm / 525 nm	N.D.	K_m =145 V_{max} =0.051 k_{cat} = 0.078	22
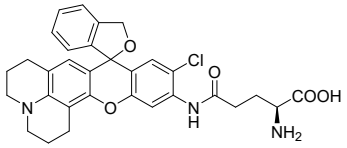	555 nm / 582 nm	N.D.	K_m =35.4 V_{max} =0.01 k_{cat} = 77.7	23
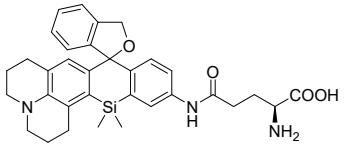	637 nm / 662 nm	N.D.	N.D.	24
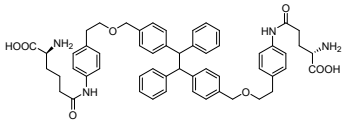	360 nm / 472 nm	0.59	K_m =15.17 V_{max} =0.018	25
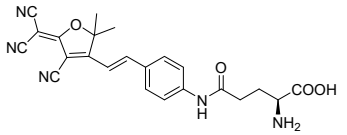	510 nm / 613 nm	0.0379	K_m =11.48	26
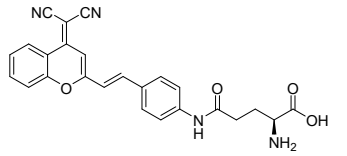	490 nm / 635 nm	0.057	K_m =10.27	27
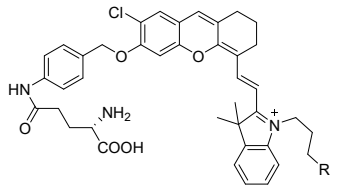 (R = c-RGD)	660 nm / 712 nm	0.0029	K_m =1.85 V_{max} =0.000109 k_{cat} = 0.005	28
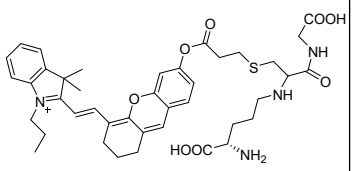	680 nm / 708 nm	0.5	K_m =7.01	29
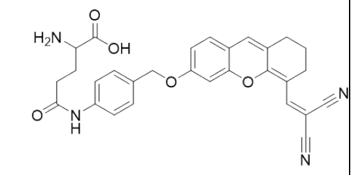	595 nm / 645 nm	0.067	K_m =21.46 V_{max} =0.0023 k_{cat} = 0.0094	This work

*N.D. Not determined.

Reference:

1. Qi, Y. H., Y.; Li, B.; Zeng, F.; Wu, S., Real-Time Monitoring of Endogenous Cysteine Levels In Vivo by near-Infrared Turn-on Fluorescent Probe with Large Stokes Shift. *Anal. Chem.* **2018,** *90* (1), 1014-1020.
2. Wu, C. X., R.; Pang, X.; Li, Y.; Zhou, Z.; Li, H., A colorimetric and near-infrared ratiometric fluorescent probe for hydrazine detection and bioimaging. *Spectrochim. Acta A Mol. Biomol. Spectrosc.* **2020,** *243*, 118764.
3. Luo, Z. F., L.; An, R.; Duan, G.; Yan, R.; Shi, H.; He, J.; Zhou, Z.; Ji, C.; Chen, H. Y.; Ye, D., Activatable Near-Infrared Probe for Fluorescence Imaging of gamma-Glutamyl Transpeptidase in Tumor Cells and In Vivo. *Chem. Eur. J.* **2017,** *23* (59), 14778-14785.
4. Reo, Y. J. D., M.; Yang, Y. J.; Ahn, K. H., Cell-Membrane-Localizing, Two-Photon Probe for Ratiometric Imaging of gamma-Glutamyl Transpeptidase in Cancerous Cells and Tissues. *Anal. Chem.* **2020,** *92* (18), 12678-12685.
5. Reo, Y. J. J., Y. W.; Sarkar, S.; Dai, M.; Ahn, K. H., Ratiometric Imaging of gamma-Glutamyl Transpeptidase Unperturbed by pH, Polarity, and Viscosity Changes: A Benzocoumarin-Based Two-Photon Fluorescent Probe. *Anal. Chem.* **2019,** *91* (21), 14101-14108.
6. Liu, H. L., F.; Wang, F.; Yu, R. Q.; Jiang, J. H., A novel mitochondrial-targeting near-infrared fluorescent probe for imaging gamma glutamyl transpeptidase activity in living cells. *Analyst* **2018,** *143* (22), 5530-5535.
7. Li, Y. X., C.; Fang, Z.; Xu, W.; Xie, H., In Vivo Visualization of gamma-Glutamyl Transpeptidase Activity with an Activatable Self-Immobilizing Near-Infrared Probe. *Anal. Chem.* **2020,** *92* (22), 15017-15024.
8.. Usama, S. M. I., F.; Kobayashi, H.; Schnermann, M. J., Norcyanine-Carbamates Are Versatile Near-Infrared Fluorogenic Probes. *J. Am. Chem. Soc.* **2021,** *143* (15), 5674-5679.
9. Liu, W. H., B.; Tong, Z.-X.; Wang, S.; Li, Y.-J.; Dai, Y.-Y., A sensitive two-photon ratiometric fluorescent probe for γ-glutamyltranspeptidase activity detection and imaging in living cells and cancer tissues. *New J. Chem.* **2018,** *42* (7), 5403-5407.
10. Liu, Y. F., B.; Cao, X.; Tang, G.; Liu, H.; Chen, F.; Liu, M.; Chen, Q.; Yuan, K.; Gu, Y.; Feng, X.; Zeng, W., A novel "AIE + ESIPT" near-infrared nanoprobe for the imaging of gamma-glutamyl transpeptidase in living cells and the application in precision medicine. *Analyst* **2019,** *144* (17), 5136-5142.
11. Hou, X. Y., Q.; Zeng, F.; Yu, C.; Wu, S., Ratiometric fluorescence assay for gamma-glutamyltranspeptidase detection based on a single fluorophore via analyte-induced variation of substitution. *Chem. Commun.* **2014,** *50* (26), 3417-3420.

12. Huo, R. Z., X.; Liu, W.; Zhang, L.; Wu, J.; Li, F.; Zhang, W.; Lee, C. S.; Wang, P., A two-photon fluorescent probe for sensitive detection and imaging of gamma-glutamyl transpeptidase. *Chem. Commun.* **2020,** *56* (74), 10902-10905.
13. An, R. W., S.; Huang, Z.; Liu, F.; Ye, D., An Activatable Chemiluminescent Probe for Sensitive Detection of gamma-Glutamyl Transpeptidase Activity in Vivo. *Anal. Chem.* **2019,** *91* (21), 13639-13646.
14778-14785.
14. Bai, B. Y., C.; Zhang, Y.; Guo, Z.; Zhu, W. H., Dual-channel near-infrared fluorescent probe for real-time tracking of endogenous gamma-glutamyl transpeptidase activity. *Chem. Commun.* **2018,** *54* (87), 12393-12396.
15. Hai, Z. W., J.; Wang, L.; Xu, J.; Zhang, H.; Liang, G., Bioluminescence Sensing of gamma-Glutamyltranspeptidase Activity In Vitro and In Vivo. *Anal. Chem.* **2017,** *89* (13), 7017-7021.
16. Li, L. S., W.; Wang, Z.; Gong, Q.; Ma, H., Sensitive fluorescence probe with long analytical wavelengths for gamma-glutamyl transpeptidase detection in human serum and living cells. *Anal. Chem.* **2015,** *87* (16), 8353-8359.
17. Wang, F. Z., Y.; Zhou, L.; Pan, L.; Cui, Z.; Fei, Q.; Luo, S.; Pan, D.; Huang, Q.; Wang, R.; Zhao, C.; Tian, H.; Fan, C., Fluorescent In Situ Targeting Probes for Rapid Imaging of Ovarian-Cancer-Specific gamma-Glutamyltranspeptidase. *Angew. Chem. Int. Ed.* **2015,** *54* (25), 7349-7353.
18. Obara, R. K., M.; Tanaka, Y.; Abe, A.; Kojima, R.; Kawaguchi, T.; Sugawara, M.; Takahashi, A.; Noda, T.; Urano, Y., gamma-Glutamyltranspeptidase (GGT)-Activatable Fluorescence Probe for Durable Tumor Imaging. *Angew. Chem. Int. Ed.* **2021,** *60* (4), 2125-2129.
19. Ou-Yang, J. L., Y.; Jiang, W. L.; He, S. Y.; Liu, H. W.; Li, C. Y., Fluorescence-Guided Cancer Diagnosis and Surgery by a Zero Cross-Talk Ratiometric Near-Infrared gamma-Glutamyltranspeptidase Fluorescent Probe. *Anal. Chem.* **2019,** *91* (1), 1056-1063.
20. Park, S. L., S.-Y.; Bae, S. M.; Kim, S.-Y.; Myung, S.-J.; Kim, H.-J., Indocyanine-Based Activatable Fluorescence Turn-On Probe for γ-Glutamyltranspeptidase and Its Application to the Mouse Model of Colon Cancer. *ACS Sens.* **2016,** *1* (5), 579-583.
21. Tong, H. Z., Y.; Zhou, L.; Li, X.; Qian, R.; Wang, R.; Zhao, J.; Lou, K.; Wang, W., Enzymatic Cleavage and Subsequent Facile Intramolecular Transcyclization for in Situ Fluorescence Detection of gamma-Glutamyltranspetidase Activities. *Anal. Chem.* **2016,** *88* (22), 10816-10820.
22. Urano, Y. S., M.; Kosaka, N.; Ogawa, M.; ; Mitsunaga, M. A., D.; Kamiya, M.; Young, M. R.; Nagano,T.; Choyke, P. L.; Kobayashi, H., Rapid Cancer Detection by

Topically Spraying a γ-Glutamyltranspeptidase–Activated Fluorescent Probe. *Sci. Transl. Med.* **2011,** *3* (110), 110-119.
23. Iwatate, R. J. K., M.; Urano, Y., Asymmetric Rhodamine-Based Fluorescent Probe for Multicolour In Vivo Imaging. *Chem. Eur. J.* **2016,** *22* (5), 1696-1703.
24. Iwatate, R. J. K., M.; Umezawa, K.; Kashima, H.; Nakadate, M.; Kojima, R.; Urano, Y., Silicon Rhodamine-Based Near-Infrared Fluorescent Probe for gamma-Glutamyltransferase. *Bioconjug. Chem.* **2018,** *29* (2), 241-244.
25. Hou, X. Z., F.; Wu, S., A fluorescent assay for gamma-glutamyltranspeptidase via aggregation induced emission and its applications in real samples. *Biosens. Bioelectron.* **2016,** *85*, 317-323.
26. Liu, F. W., Z.; Wang, W.; Luo, J. G.; Kong, L., Red-Emitting Fluorescent Probe for Detection of gamma-Glutamyltranspeptidase and Its Application of Real-Time Imaging under Oxidative Stress in Cells and in Vivo. *Anal. Chem.* **2018,** *90* (12), 7467-7473.
27. Zhang, P. J., X. F.; Nie, X.; Huang, Y.; Zeng, F.; Xia, X.; Wu, S., A two-photon fluorescent sensor revealing drug-induced liver injury via tracking gamma-glutamyltranspeptidase (GGT) level in vivo. *Biomaterials* **2016,** *80*, 46-56.
28. Luo, Z. H., Z.; Li, K.; Sun, Y.; Lin, J.; Ye, D.; Chen, H. Y., Targeted Delivery of a gamma-Glutamyl Transpeptidase Activatable Near-Infrared-Fluorescent Probe for Selective Cancer Imaging. *Anal. Chem.* **2018,** *90* (4), 2875-2883.
29. Li, L. S., W.; Wu, X.; Gong, Q.; Li, X.; Ma, H., Monitoring gamma-glutamyl transpeptidase activity and evaluating its inhibitors by a water-soluble near-infrared fluorescent probe. *Biosens. Bioelectron.* **2016,** *81*, 395-400.